Final Report
FHWA-SC-19-04

Deep Soil Test Borings to Determine Shear Wave Velocities Across South Carolina

Sponsoring Agencies:
South Carolina Department of Transportation

Federal Highway Administration

Principal Investigators:
Dr. Inthuorn Sasanakul
Civil and Environmental Engineering
University of South Carolina
Dr. Sarah Gassman
Civil and Environmental Engineering
University of South Carolina

October 2019

Technical Report Documentation Page

1. Report No. FHWA-SC-19-04	2. Government Accession No.	3. Recipient's Catalog No.
4. Title and Subtitle Deep Soil Test Borings to Determine Shear Wave Velocities Across South Carolina		5. Report Date October 2019
		6. Performing Organization Code
7. Author(s) Inthuorn Sasanakul, Sarah Gassman		8. Performing Organization Report No.
9. Performing Organization Name and Address University of South Carolina Civil and Environmental Engineering 300 Main St., Columbia, SC 29208		10. Work Unit No. (TRAIS)
		11. Contract or Grant No. SPR No. 731
12. Sponsoring Agency Name and Address South Carolina Department of Transportation PO Box 191 Columbia, SC 29202-0191		13. Type of Report and Period Covered Final Report
		14. Sponsoring Agency Code
15. Supplementary Notes Pitak Ruttithivaphanich and Siwadol Dejphumee		

16. Abstract

Having an accurate shear wave velocity profile and a better understanding of dynamic behavior of the deep soil deposits in the South Carolina Coastal Plain are critical for seismic hazard analyses of critical transportation infrastructure. This research presents a study that obtained comprehensive field and laboratory measurements of shear wave velocity and dynamic soil behaviors for two sites in the South Carolina Coastal Plain where data was limited. Site A is located near Conway in Horry County and Site B is located in Andrews in Williamsburg County. Geotechnical borings were drilled at these two locations to depths of 505 and 615 ft to perform extensive geotechnical and geological site characterization. Shear wave velocity profiles were developed using several geophysical testing methods including P-S suspension logging, full waveform sonic logging, a combined multi-channel analysis of surface waves and spectral analysis of surface waves, and a combined multi-channel analysis of surface waves and microtremor array measurement methods. The developed profiles were compared, and similarities and differences were discussed in this report.

Shear modulus and damping behaviors over a wide range of strains for soil and rock samples collected from both sites were evaluated using resonant column and torsional shear methods. It was found that the behaviors of materials obtained from Tertiary and Cretaceous deposits deviated from the empirical predictions based on plasticity index and geologic age. Based on the results, the predictive curves for shear modulus and damping curves are not recommended for older soil deposits, particularly for those samples with cementation.

17. Key Word	18. Distribution Statement		
Shear Wave Velocity, Shear Modulus, Damping Site Response Analysis, Geophysical Test, Resonant Column Test, Torsional Shear Test	No restrictions.		
19. Security Classif. (of this report)	20. Security Classif. (of this page)	21. No. of Pages	22. Price
Unclassified.	Unclassified.	621	

Disclaimer

The contents of this report reflect the views of the author who is responsible for the facts and the accuracy of the data presented. The contents do not necessarily reflect the official views of the South Carolina Department of Transportation or Federal Highway Administration. This report does not constitute a standard, specification, or regulation.

The State of South Carolina and the United States Government do not endorse products or manufacturers. Trade or manufacturer's names appear herein solely because they are considered essential to the object of this report.

Acknowledgments

This project was funded by the South Carolina Department of Transportation and the Federal Highway Administration under grant SPR 731. Their support is greatly appreciated.

The authors would like to acknowledge personnel from the South Carolina Department of Transportation for their assistance throughout the project. The SCDOT research development personnel included: Terry Swygert and Meredith Heaps. The implementation committee of this project included: Nicholas Harman, Jeremy Harmon, Bill Jones, Trapp Harris, Renee Gardner, and Blake Gerken (FHWA), and Ani Garignan and Emad Ghebi formerly with SCDOT.

The authors would like to express special thanks to the following individuals who provided support to this project.

William (Billy) Camp	S&ME
Kyle Murrell	S&ME
Levi Ekstrom	S&ME
Christopher Stryffeler	formerly with S&ME
Brady Cox	UT Austin
Antony Martin	GEOVision
John Diehl	GEOVision
Scott Howard	SCDNR
Joe Gellici	SCDNR
William Doar	SCDNR
Michael Waddell	USC
Camille Ransom	SCDHEC
Joy McLaurin	Farmers Grain & Milling

Finally, the authors would like to thank the staff and students at the University of South Carolina for their administrative and technical support of this project. The following graduate students; Pitak Ruttithivaphanich, Siwadol Dejphumee, William Ovalle Villamil, and Kazi Islam assisted with field measurements, laboratory testing, and data compilation and analysis. The following undergraduate students; Veronica Bense, Nicolet Chavancak, Ryan Devine, Javonte Isaac, E'Lexus Nelson, and Bryce Reeve, assisted with laboratory testing.

Executive Summary

This report presents the findings from a study undertaken to obtain deep soil profiles at two sites in the South Carolina Coastal Plain. Site A is located near Conway in Horry County and Site B is located in Andrews in Williamsburg County. Geotechnical borings were drilled to depths of 505 and 615 ft for Sites A and B, respectively. Shear wave velocity profiles were generated using P-S suspension logging, full waveform sonic logging, combined multi-channel analysis and spectral analysis of surface waves (MASW-SASW), and combined multi-channel analysis of surface waves and microtremor array measurement (MASW-MAM) methods. Soil and rock samples were collected for further characterization in the laboratory. Resonant column and torsional shear testing methods were utilized to evaluate dynamic soil behaviors for a wide range of strains.

The shear wave velocity profiles using P-S suspension logging were obtained to a depth of 470 ft for Site A and a depth of 600 ft for Site B. Profiles to a depth of 220 ft were obtained from the MASW-SASW method for both sites. For the combined MASW-MAM method, profiles were obtained to a depth 4921 ft for Site A and a depth of 2625 ft for Site B. Overall, the average shear wave velocities obtained from the surface methods within the top 200 ft were lower than that of the P-S suspension logging data. This resulted in a different NEHRP site class when using the average shear wave values in the top 100 ft for Site A, but not site B. The P-S suspension logging provided detailed characteristics of the soil profile and the results agreed with the visual observation of samples. However, the P-S suspension logging method did not provide the depth of the B-C boundary, as the boundary was below the bottom of each borehole.

The results from both surface methods were in agreement within the top 220 ft where the MASW-SASW results could be compared. The MASW-MAM method is a unique method utilizing passive ambient wave sources and specialized sensors that allows deep profiling and identified an estimated depth to the B-C boundary of 580 ft for Site A and 1343 ft for Site B. Results from both surface methods show that spatial variation of both sites are high, especially for Site A. The shear wave profiles from the surface wave methods represent the average profiles over a large volume of soil; whereas, the profiles from the borehole methods represent localized profiles within the tested borehole. Results from the different methods provide understanding of the range of uncertainty in the shear wave velocity profiles that should be accounted for when performing site response analysis.

Visual observation of samples collected from both sites showed that materials were highly variable with frequent transitions between soil-like to rock-like material. Highly cemented sand or clay with thicknesses varying from a few inches to several feet depth were observed at several depths throughout the soil profiles. The location of these rock-like materials corresponded with the high shear wave velocities observed from the P-S logging profile.

Many soil and rock samples were tested to evaluate dynamic soil behaviors, specifically to determine the variation of shear modulus and damping for a wide range of strains. Overall, it was found that the material behaviors deviate from the predicted behaviors obtained based on soil index properties and geologic age provided in the literature. Relatively high damping values were observed particularly at low strains and the values were significantly affected by loading frequency applied using different testing methods. The effect of soil plasticity in relation to geologic age was evaluated for the shear modulus and damping relations, and no clear trend was observed for Tertiary and Cretaceous soil deposits. As a result, the shear modulus and damping behaviors were not accurately predicted for these soils. It is hypothesized that cementation is likely to be a significant factor affecting the dynamic soil behavior; however, detailed evaluation of cementation in relation to shear modulus and damping was beyond the scope of this study.

Data from this study can be used directly to perform site-specific site response analysis for the sites studied herein with the recommendation to perform sensitivity analyses to account for uncertainty in the shear wave velocity profiles, depth of competent rock, dynamic soil behavior, and impacts of interbedded rock and cemented layers. Predictive equations found in the literature for shear modulus and damping curves are not recommended for Tertiary and Cretaceous deposits because this study showed that soil plasticity and geologic age alone are not dominant factors for older soil deposits, particularly for those samples with cementation.

Table of Contents

List of Figures

List of Tables

1. Introduction

The South Carolina Coastal Plain consists of a deep soil basin with variable thicknesses of sedimentary deposits across the area. The deep soil basin condition, where the depth to the top of rock is greater than 500 ft, is not properly described by the National Earthquake Hazards Reduction Program (NEHRP) site coefficient, thus site-specific site response analysis (SSRAs) is typically required to determine the design response spectra for structures situated on deep soil basin sites. Shear wave velocity (V_s) profiles, the depth of soil sediment to the top of soft rock (i.e., the B-C boundary), and the variation of soil modulus and damping with shear strain are the primary inputs for site response analysis. These parameters have significant impacts on the results of SSRAs.

The overall goal of this research was to reduce uncertainties in SSRAs for the South Carolina Department of Transportation (SCDOT) seismic design. The research goal was achieved through extensive field and advanced laboratory investigations of deep V_s profiles for two sites in South Carolina. The research presented herein is the first geotechnical and geological investigation where several field methods were used and advanced laboratory testing was performed. The research developed a set of high quality geotechnical and geophysical data as well as geological information that can be used to perform SSRAs and can be used to further interpret other sites in the Coastal Plain.

Two sites located in the South Carolina Coastal Plain were identified by the SCDOT where the deep V_s profiles and geological information were very limited and/or not available. Site A is located near Conway in Horry County and Site B is located in Andrews in Williamsburg County. The target depth of borehole was approximately 500 and 600 ft deep for Site A and Site B, respectively. Borehole geotechnical and geophysical methods were performed to characterize soil and rock properties and develop the V_s profiles. These profiles were compared with the V_s profiles developed from non-invasive surface geophysical methods to evaluate differences in testing methods.

1.1. Research Objectives

The research program was designed to accomplish the following objectives:

1. Conduct geotechnical field exploration at two sites and develop comprehensive soil boring logs;
2. Conduct field geophysical testing using different methods at two test sites to develop shear wave velocity profiles and compare the similarities and differences between these profiles;
3. Collect soil and rock samples and conduct a series of geotechnical laboratory tests to determine the physical, mechanical and small strain dynamic properties of the materials in accordance with applicable ASTM and AASHTO standards; and
4. Evaluate parameters that are useful for SSRAs to be conducted for future SCDOT projects at these two sites. These parameters include: average shear wave velocity in the top 100 ft (V_{s100ft}), depth to the top of soft or competent rock (i.e., the B-C

boundary), and representative normalized shear modulus (G/G_{max}) and damping (D) curves. These parameters are compared with the database currently available to SCDOT engineers and contractors.

1.2. Research Tasks

To meet the objectives, the project was divided into four work tasks spanning a 33-month period. The tasks are listed as follows:

Task 1: Preparation of field and laboratory testing program
Task 2: Field investigation
Task 3: Laboratory testing of soils and rocks
Task 4: Final data compilations and documentation

1.3. Organization of The Report

This report has been organized into five chapters including the introduction to the project presented here. Chapter 2 presents the background of this project. Chapter 3 presents methodology used for Tasks 2 and 3. The results and analysis are presented in Chapter 4, including key findings and comparisons of V_s profiles generated from different methods and geotechnical and geological boring logs, small strain dynamic properties of soil and rock samples and factors affecting the small strain dynamic properties and comparisons of results with empirical relationships, and a new relationship proposed for Cretaceous age deposits. Chapter 5 presents conclusions, recommendations, and the implementation plan. Appendices A-G include all of the data and detailed information necessary for the report.

2. Background

The Atlantic Coastal Plain is a geological condition found in the Central and Eastern United States. The coastal plain consists of unconsolidated sediments as thick as 3,000 ft underlain by very hard rock with shear wave velocity, V_s of over 8500 ft/s. In South Carolina, this very hard rock layer is located close to or at the ground surface in Columbia and its depth increases toward the coast as well as increasing in depth from North to South (Chapman and Talwani 2002). The deep sediments consist of unlithified sediments with weakly lithified units that are formed during Cretaceous, Tertiary (Neogene and Paleogene period), and Quaternary periods (Chapman et al. 2006). Many geologic formations have been identified within the SC Coastal Plain and a wide variety of materials were found within these formations, including sand, clay, gravel, limestone, and marl (SCDNR 2005). This unique geological and geotechnical condition poses significant challenges to seismic hazard analyses for the South Carolina Coastal Plain.

A V_s profile of soil sediment to the top of "competent" rock (a boundary defined as having a V_s of 2500 ft/s) and associated dynamic properties (i.e. shear modulus reduction and damping curves) are important parameters for seismic hazard analyses (Kavazanjian et al. 1997). In the Western United States, where most of the current seismic design criteria have been developed, the top of the competent rock is relatively shallow; hence the required V_s profile is typically no more than 100 ft deep. In the South Carolina Coastal Plain, the depth to the top of competent rock can be much deeper than 100 ft. The sediment from the ground surface to the top of competent rock typically consists of sediment deposits composed of complex layers of materials at different stages of the chemical weathering process. Due to limited data availability for the dynamic properties of the South Carolina Coastal Plain and high cost in site investigation, geotechnical engineers are required to account for high level of uncertainty for the design.

Andrus et al. (2014) compiled V_s profiles obtained from the literature for several locations in South Carolina. These profiles were measured by different borehole and non-intrusive geophysical methods. Ranges of shear wave velocity were correlated with geological units. An average V_s of approximately 623 ft/s was recommended for the Quaternary deposit, and 1312-2100 ft/s was recommended for the Tertiary deposit. The top of rock (i.e., B-C boundary) was defined where the V_s was greater than 2500 ft/s for the Tertiary and older deposits. The V_s data for the Cretaceous deposit was very limited and typically assumed to be higher than 2500 ft/s. Representative V_s profiles suggested by Andrus et al. (2014) for the Charleston-Savannah and Myrtle Beach areas are shown in Fig. 2.1. They were developed by averaging several V_s profiles obtained primarily for depths no deeper than 100 ft. Available V_s data at depths greater than 100 ft were limited to a few locations. Therefore, additional V_s data at deeper depths are needed for the South Carolina Coastal Plain in order to reduce uncertainties in estimating V_s for different soil types and geological formations as well as the estimated depth to the top of competent rock.

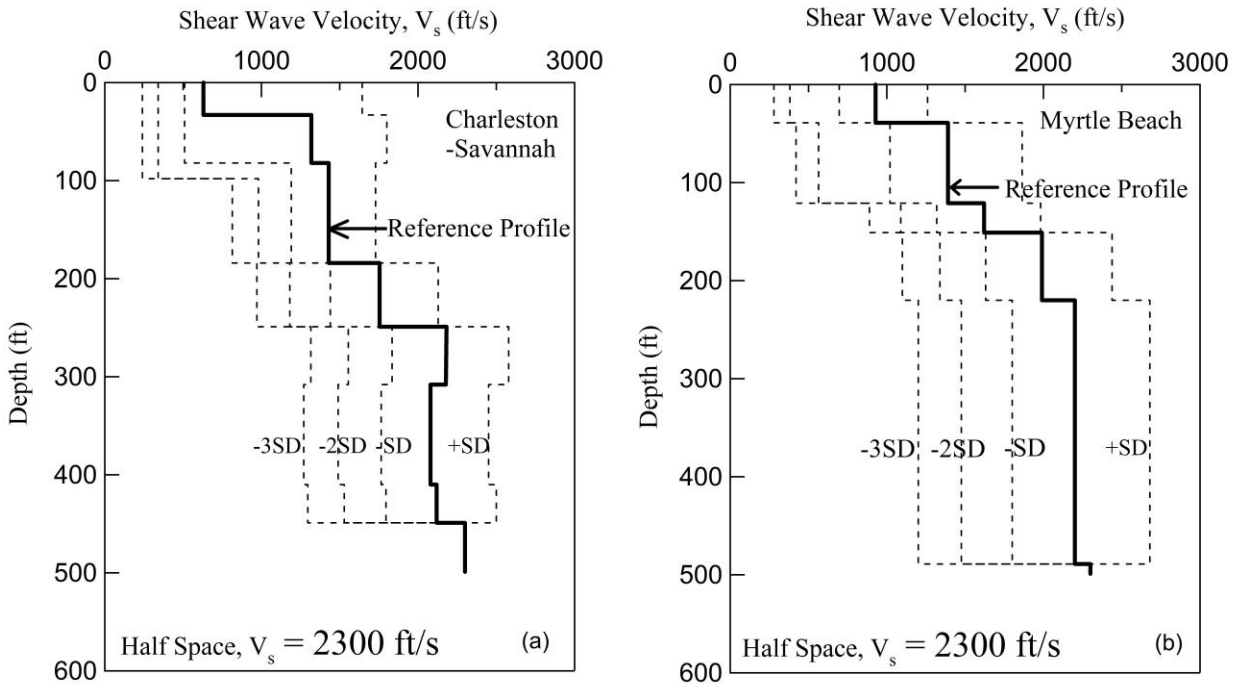

Figure 2.1 Shear Wave Velocity Profiles for (a) Charleston-Savannah and (b) Myrtle Beach (adapted from Andrus et al. 2014)

Recently, additional deep soil boring investigations have been performed for several projects in the South Carolina Coastal Plain (i.e., GeoVision 2008, GeoVision 2010, S&ME 2015, and F&ME 2017); however, compared to other areas of the world with seismic hazards, practitioners in South Carolina face significant challenges due to lack of data (e.g., recorded ground motions, and deep geotechnical boreholes) and the unique geological conditions (e.g., deep unlithified sediments) that are different than the sites in the Western United States where a large amount of data has been used to develop the USGS simplified procedure. A sensitivity analysis is typically performed to address some of the uncertainties in the site response analysis, but there is no consensus or guidance on how to address these uncertainties or quantify the impact of the assumptions (Camp 2018).

In addition to the V_s profiles, the variation of shear modulus and damping with shearing strain are important inputs for site response analysis. Andrus and his colleagues (Andrus et al. 2003, Zhang et al. 2005, and Zhang et al. 2008) developed predictive equations for estimating the normalized shear modulus (G/G_{max}) and damping (D) for South Carolina soils based on geologic age, confining pressure, and soil plasticity. Results were compiled from resonant column and torsional shear tests from 122 soil specimens, 78 of which were from three locations in South Carolina (see Fig. 2.2). The previous study indicated that the geologic age and confining pressure have a larger impact on small strain dynamic properties than soil plasticity. They also reported that Quaternary-age soil dynamic behavior is more linear than Tertiary soil and residual/saprolite soil. This

approach is useful for an estimation of G/G_{max} and D variation over a range of strain when laboratory testing is not possible. However, more data are needed for strata deeper than 100 ft, particularly for older deposits (e.g. Tertiary and Cretaceous soil) and other geologic formations for the SC Coastal Plain. Recently, additional G/G_{max} and D data for soils in the lower Coastal Plain were obtained by S&ME (2015) and F&ME (2017), thus there is a need to update the Andrus et al. (2003) database and the associated prediction model. Currently, due to a large variation of material properties in the SC Coastal Plain, the site response analyses are performed using both predicted curves proposed by Andrus et al. (2003), or generic curves available in the literature. The generic curves were typically developed from uncemented sand or clay and the confining pressure and plasticity index generally governs dynamic soil properties (e.g. Vucetic and Dobry 1991, Seed et al. 1986, Sun et al. 1988, Ishibashi and Zhang 1993, and Darendeli 2001).

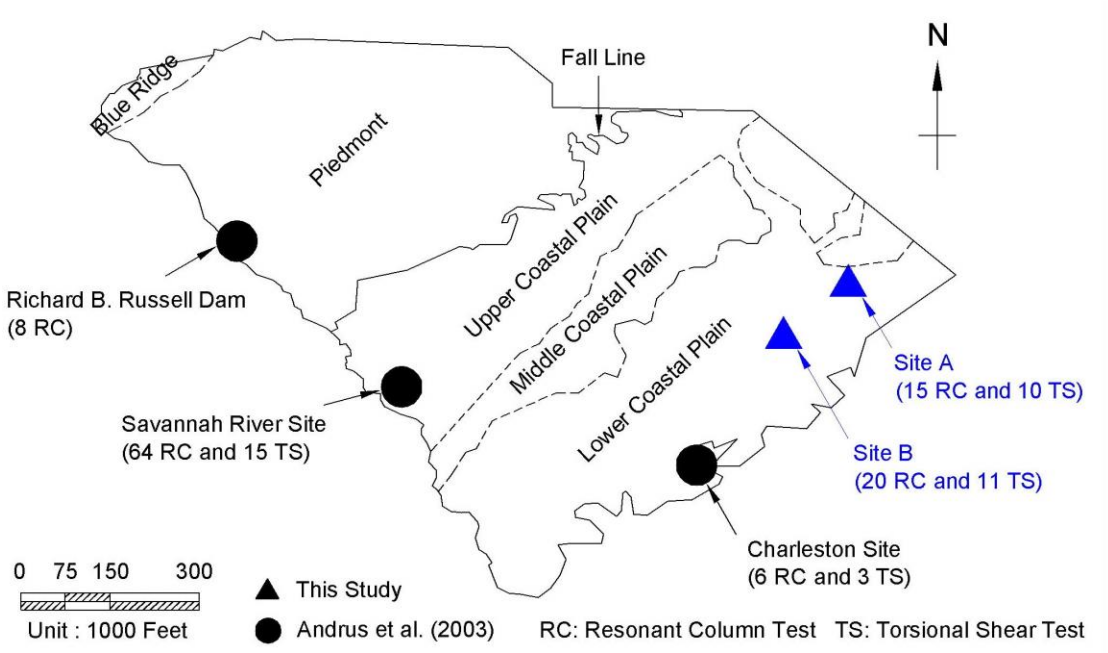

Figure 2.2 Locations of Soil Specimens from Zhang et al. (2005) and this Study (labeled as Site A and Site B) (adapted from Zhang et al. 2005)

3. Methodology

This chapter presents a summary of the methodology used for characterizing deep shear wave velocity profiles and dynamic soil properties. More detailed information can be found in the Appendices.

3.1. Sites Studied and Project Team

Two sites in South Carolina were selected as shown in Fig. 3.1. Site A is located near Conway in Horry County. Site B is located in Andrews in Williamsburg County. The sites are located in the Lower Coastal Plain and were chosen because deep soil borings have not been performed in these areas and the V_s profiles and dynamic soil properties were unknown. To obtain the V_s profiles and define the depth to the top of competent or soft rock (V_s = 2500 ft/s), several geophysical testing methods were used: P-S suspension logging, full waveform sonic logging (FWS), a combined multi-channel and spectral analysis of surface waves (MASW-SASW) method, and a combined multi-channel analysis of surface waves and microtremor array measurement (MASW-MAM) method. Soil and rock samples were collected and tested in the laboratory to obtain small strain dynamic properties using resonant column (RC) and torsional shear (TS) methods. The success of this project required effective coordination and execution of the field exploration, geophysical testing activities, and specialized laboratory testing. An organizational chart showing the project team is presented in Fig. 3.2.

Figure 3.1 Study Sites

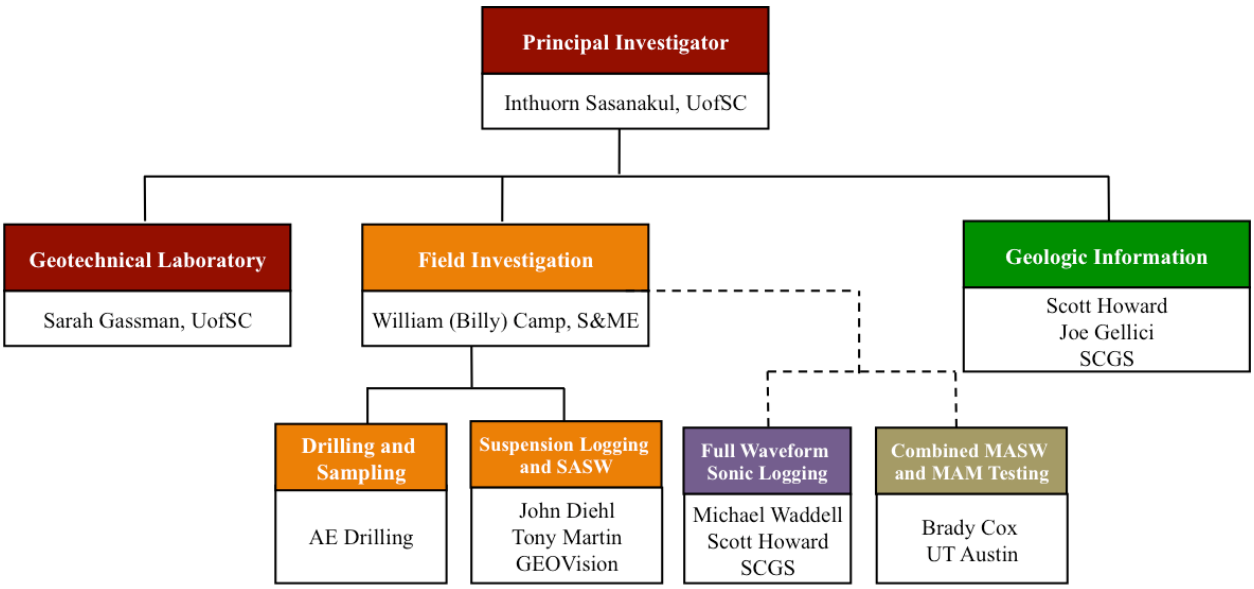

Figure 3.2 Project Organizational Chart

3.2. Field Investigation

3.2.1. Borehole Geotechnical Investigation

The geotechnical borings were drilled by AE Drilling under the supervision of S&ME. The methods utilized a combination of mud-rotary drilling, in general accordance with ASTM D5783, and wireline coring procedures, in general accordance with ASTM D2113. Each borehole was approximately 6-inch in diameter to allow for insertion of the geophysical testing equipment. Standard Penetration Test (SPT) split-barrel (split-spoon) sampling and/or thin-walled (Shelby) tube sampling were performed continuously from the ground surface until hard materials (i.e. SPT N-value is over 50 blows per ft) were consistently encountered. SPT split-barrel tube sampling was performed in general accordance with ASTM D1586/D1586M. In SPT sampling, a standard 2-inch diameter split steel tube was driven into undisturbed soil at a select depth using a 140-lb hammer falling a distance of 2.5 ft. The number of blows required to drive the sampler each 6-inch interval was recorded. The N-value represents the number of blows required for 1-foot penetration into the soil after an initial 6 inch "seating" drive depth was recorded. In this study "continuous" 2 ft interval SPT sampling was performed. Field logging was performed in general accordance with ASTM D5434. As the split-barrel samples were collected, visual classification of the soil was performed in general accordance with ASTM D2488 and the samples were then sealed in plastic bags.

Shelby tube sampling was performed in general accordance with ASTM D1587/D1587M. Several Shelby tube samples were collected from both sites. In cases where damage to the Shelby tube sample was considered likely, a pitcher-barrel sampler was used to attempt the sample. A pitcher-

barrel sampler consists of a spring-mounted, 2.5 ft long, thin-walled tube inner barrel with a rotating exterior cutting shoe/barrel. When used in softer materials the spring extends the tip of the thin-walled tube beyond the cutting shoe to collect the sample. In stiffer materials the spring is compressed which results in the cutting shoe leading the thin-walled tube as it is advanced. The recovered tube samples were cleaned at each end, and then sealed with wax in general accordance with ASTM D4220/D4220M.

Once hard material was consistently encountered, the mud-rotary tooling was replaced with H-sized soil/rock coring tools. Coring was accomplished by advancing an outer steel casing with rock carbide or diamond bit, and an inner sample barrel that was locked into the drill string annulus. A triple-tube split inner barrel wireline coring system was used in an effort to enhance core recovery. Once implemented, continuous core runs were conducted at 5 ft intervals. The core samples were collected and visually classified in general accordance with ASTM D2488. The samples were then wrapped in cellophane and placed in polyurethane lined wooden boxes, which were then labeled and prepared for transportation. This procedure was continued until the borehole termination depth was reached. At the termination depth, the borehole was flushed until the geophysical testing was ready to begin logging, at which point the drillers removed tooling and P-S suspension logging commenced.

3.2.2. P-S Suspension Logging Method

The P-S Suspension Logging was performed by GEOVision in general accordance with the procedure outlined in Appendix A. This method is a borehole geophysical method performed by lowering a probe into an open, fluid-filled borehole. The probe measured approximately 25 ft long and included a combined reversible polarity solenoid horizontal shear-wave source and compressional-wave source, which was paired with two biaxial receivers and separated by a flexible isolation cylinder. The receiver pair was centered approximately 12.5 ft above the bottom end of the probe and the receivers were located 1 m apart. The probe was suspended by an armored, multi-conductor cable that was wound about the drum of a winch. The winch was used to meter the cable travel as the probe was lowered into the fluid-filled borehole. The source was triggered after the probe was lowered in 1.5 ft increments.

Pressure waves generated by the source propagated horizontally outward into the fluid surrounding the probe. When the pressure wave impacted the borehole wall, it was converted to compression and shear waves that travel along the length of the borehole wall and convert back to pressure waves near the two biaxial receivers. The system recorded the time it took for the compression and shear waves to reach the two receivers. As the testing was conducted, the operator observed the recorded data and adjusted the gains, filters, delay time, pulse length, and sample rate to improve the quality of the data being recorded.

The recorded data was digitally processed to separate the compression and shear waves using different filtering techniques, such as adjusting the filter frequency and applying Digital Fast Fourier Transform - Inverse Fast Fourier Transform low-pass filtering. The compression and shear

wave velocities were calculated from the distance and time of travel for each waveform from source to receiver 1, and from receiver 1 to receiver 2. These velocities were plotted against the depth of each testing interval.

3.2.3. Full Waveform Sonic Logging Method

The FWS logging was performed by a team from the South Carolina Geological Survey (SCGS), Department of Natural Resources. Similar to the P-S Suspension Logging method, this method was performed by lowering a FWS tool into an open, fluid-filled borehole (Minear 1986). The FWS tool consists of one transmitter and three to four receivers. The transmitter generates source waves and the receivers record four types of waves: compression wave (P-wave), shear wave (s-wave), pseudo Rayleigh wave, and Stoneley wave. In this study, the Mount Sopris 2SAA-1000/F-FWS probe with two transmitters and three receivers were used to acquire the shear wave data at 0.5 ft intervals with a logging rate of 10 ft/min. During acquisition, the in-coming waveforms from each receiver at every sample interval were recorded for real-time analysis by WellCAD® software. The logging rate and cable tension were constantly monitored to ensure quality control on the incoming signals, alert the operator if there was a problem with the tool, and maintain data quality. Semblance Analysis was used to determine P-wave and shear wave velocity (Kimball et al. 1984). More detailed information about the FWS logging method can be found in Appendix C.

3.2.4. Combined Multi-Chanel Analysis and Spectral Analysis of Surface Waves (MASW-SASW) Method

The combined MASW-SASW test was performed by GEOVision. Both MASW and SASW methods were performed utilizing a series of receivers in linear arrays recording data simultaneously during dynamic loading at the surface. The MASW method collects multi-channel seismic data while the SASW method collects surface wave phase data traveling from the source to each receiver. Both methods used a linear array of geophone receivers that were setup to record surface waves traveling from the source to each receiver (e.g. Rix et al. 1991 and Stokoe et al. 1994). Multiple linear arrays incorporating different receiver spacing and locations were used to analyze surface waves of differing wavelengths and frequencies. The Rayleigh and Love waves generated by the sources travel at similar speeds to shear waves and can therefore be used to estimate a representative shear wave velocity for individual layers of soil or rock. Rayleigh waves were measured using a vertical source and an array of vertical receivers, and were representative of vertically polarized shear waves as they traveled through a layered medium. Love waves were measured using a horizontal source and an array of horizontal receivers oriented perpendicular to the orientation of the linear array and were representative of horizontally polarized shear wave as they traveled through a layered medium. Both methods generate dispersion curves and data modeling is performed to obtain the V_s profile. Depending upon the dispersive nature of the Rayleigh and Love waves traveling along a layered medium, reflecting and refracting off separate layers, each waveform creates small differences in the return time. Electrical impulses were generated as waves passed each receiver location and were stored for each dynamic load session.

Dynamic loads for these techniques typically range from small hammers and sledgehammers to accelerated weight drops and movement of heavy equipment. Resolution of the wave data was heavily dependent on the precision of the array layouts and how well the receivers were coupled to the exposed surface.

In addition to a sledgehammer, a Caterpillar 336F excavator (bucket drop and moving back and forth in place) was used as the energy source to extend the depth of investigation to 200 ft, or greater. Both 1 and 4.5 Hz geophones were used. The MASW data were acquired along three collocated arrays. Two arrays used 48 vertical 4.5 Hz geophones spaced 5 and 10 ft apart, respectively and one array used 9 vertical 1 Hz geophones with variable spacing. The length of the arrays for each site was different and ranged from 230 to 490 ft. Depending on the site, type of energy source, and geophone arrays, the source-receiver offset ranged from 5 to 295 ft. The SASW data were acquired along a single array at each site. For SASW, the 1 Hz vertical geophones were used with several receiver spacings that ranged from 148 to 394 ft the MASW-MAM arrays are shown in Figs. 3.3(a) and 3.4(a) for Site A and Site B, respectively.

The SASW dispersion curves were generated using the software WinSASW V3 and were combined with the MASW dispersion curves generated using the software Seismic Pro Surface V8.0 for both sites. The representative Rayleigh wave dispersion curve was modeled using forward and/or inverse modeling in the software Seisimager to develop several V_s models corresponding to different receiver spacing. During this process an initial velocity model generated based on soil boring logs and the iterative process of forward or inverse modeling is performed until a V_s model with low root mean square error (RMS) between the theoretical and experimental dispersion data is developed. More detailed information can be found in Appendix A.

3.2.5. Combined Multi-Channel Analysis of Surface Waves (MASW) and Microtremor Array Measurement (MAM) Method

The combined MASW-MAM method was performed by a team led by Dr. Brady Cox from the University of Texas at Austin. The MASW method was performed using the same procedure as the combined MASW-SASW; however, a sledgehammer was used as the source, different arrays of geophones were used, and the source-receiver offset ranged from 16 to 65 ft from the end of geophone array.

For the MAM method, three-component broadband seismometers were used to record ambient vibrations. The MAM testing at Site A was performed using two roughly-triangular arrays and one circular array as shown in Fig. 3.3(b). Each array utilized ten three-component seismometers, resulting in a maximum array spacing of 164, 984, and 3937 ft for the inner circular array and two outer triangular arrays, respectively. The MAM testing at Site B was performed using three nested circular arrays as shown in Fig. 3.4(b). Ten seismometers were incorporated in the 164 ft and 1492 ft arrays and eight seismometers were in the 1476 ft array.

From the MAM arrays at both sites, all of the data recorded at each seismometer station were computed to generate the representative horizontal to vertical (H/V) spectral ratios curves. The inversion process was performed using a multi-mode approach by matching various combinations of fundamental, first higher, second higher, and other Rayleigh and Love modes to the experimental dispersion data. The inversion was performed using the Software Geopsy by applying the neighborhood algorithm to locate earth models within a pre-defined parameterization that yield the lowest possible misfit values between the theoretical and experimental data. In this study, about 500,000 to 750,000 trial layer earth models for each distinct parameterization was used to obtain a large number of acceptable models controlled by the experimental data and model parameterization. The inverse process resulted in over 100 V_s profiles associated with theoretical dispersion curves from each acceptable inversion parameterization obtained from soil boring logs for both sites. In this study, the median V_s profiles are obtained and recommended for each site. More detailed information can be found in Appendix B.

Figure 3.3 Surface Geophysical Testing Locations at Site A: (a) MASW and SASW Testing Arrays, (b) MASW and MAM Testing Arrays

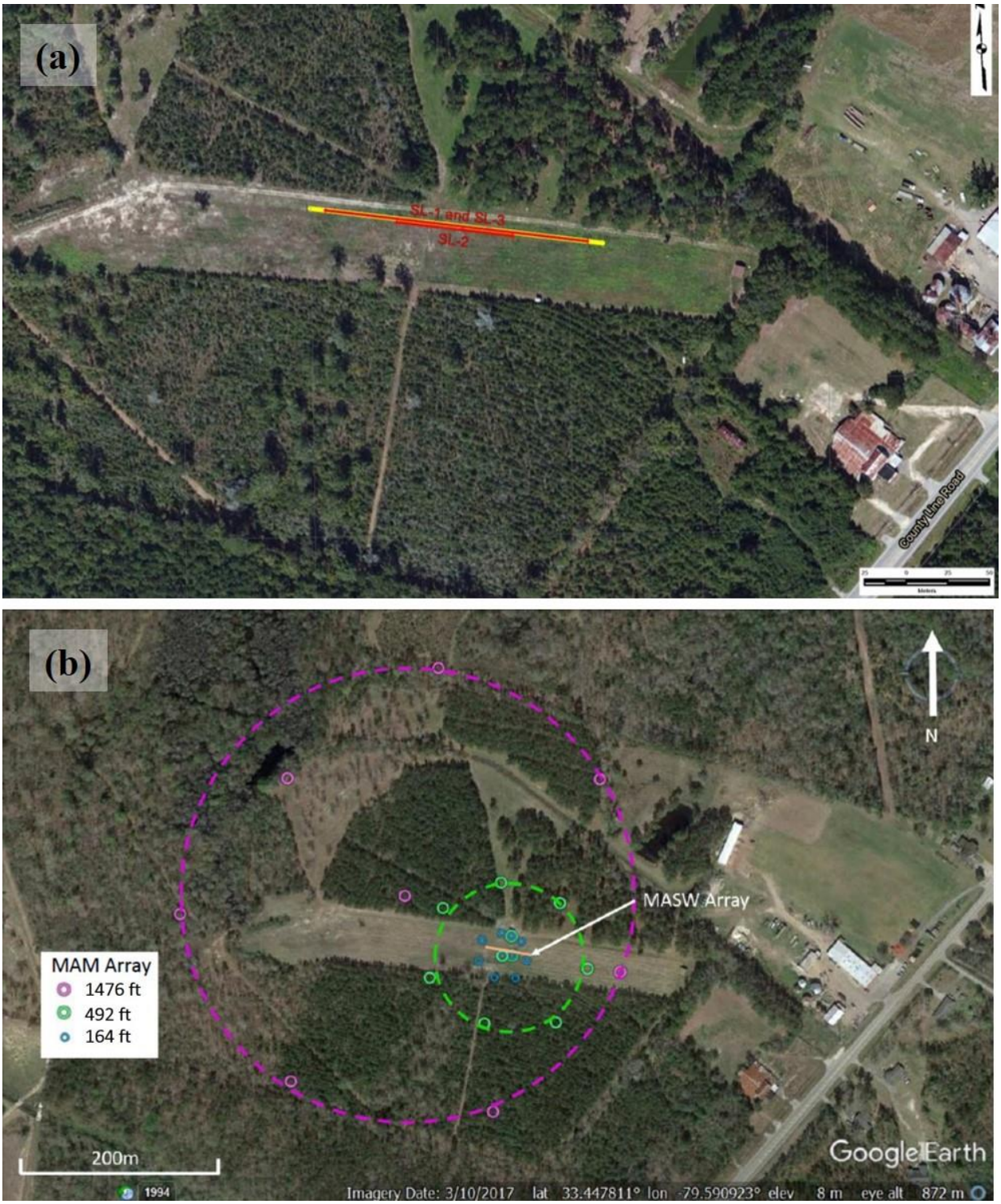

Figure 3.4 Surface Geophysical Testing Locations at Site B: (a) MASW and SASW Testing Arrays, (b) MASW and MAM Testing Arrays

3.3. Laboratory Testing of Soils and Rocks

Following completion of the field investigation, samples were transported in secure containers to the Geotechnical Laboratory at the University of South Carolina. A summary of the laboratory testing is presented in Table 3.1. Testing methods are described as follows.

Table 3.1 A Summary of Laboratory Testing of Soil and Rock Samples

Analysis	Standard Method	Parameter	Number of Tests
Identification			
Description and Identification of Soils (Visual-Manual Procedure)	ASTM D2488	Angularity, shape, color, moisture condition, consistency, etc	221
Classification of Soils for Engineering Purposes AASHTO Unified Soil Classification System (USCS)	 AASHTO M 145-87 ASTM D3282 ASTM D2487	 Soil Type	 221
Index Properties			
Moisture Content of Soil and Rock	ASTM D 2216	w_n	223
Liquid Limit, Plastic Limit, and Plasticity Index of Soils	ASTM D 4318	LL, PL, PI	191
Grain Size Analysis (Sieve Analysis) Wash Sieving	ASTM D 422 ASTM D 6913 ASTM D 1140-17	C_u, C_c, D_{10}, D_{50}, % fines	221
Specific Gravity (rock samples only)	ASTM C 127-88 AASHTO T 85-91	G_s	15
Dynamic Soil and Rock Properties			
Resonant Column Test	ASTM D 4015	G,D	35
Torsional Shear Test	n/a	G,D	21

3.3.1. Geological Logging

Geological logging of the core samples was performed by Mr. Joe Gellici, professional geologist from the South Carolina Geological Survey, Department of Natural Resources. A detailed description of the core samples can be found in Appendix D. The results were correlated with geophysical logs (gamma-ray logs), visual observation of core samples, and formations determined at other core holes in the same area in an attempt to determine the geological formation associated with each of the core samples.

3.3.2. Soil Classification and Index Property Measurements

Each sample was visually classified and measurements of index properties were performed in the Geotechnical Laboratory at the University of South Carolina according to the ASTM standards provided in Table 3.1. The USCS symbols and index properties were used to update the geotechnical boring logs provided by S&ME.

3.3.3. Small Strain Dynamic Properties Measurements

Following completion of the field sample collection, selected core samples were carefully wrapped and sealed to preserve the moisture content and then stored prior to laboratory testing. The samples obtained from the Shelby tube and core samplers were tested for dynamic soil properties using the resonant column (RC) method according to ASTM D4015 and the torsional shear (TS) method. An ASTM standard for the TS test does not exist currently, but this test method is well established (e.g., Kim 1991 and Sasanakul 2005). Both RC and TS methods are the most widely used methods to evaluate modulus reduction (G/G_{max}; G_{max} is low-strain shear modulus) and damping over a range of strains for soils. These tests require highly specialized skills and experience. A more detailed description of the sample preparation and RC/TS testing procedure can be found in Appendix F.

A Stokoe-type RC/TS apparatus located in the Geotechnical Laboratory at the University of South Carolina was used in this project. This type of apparatus has been used world-wide for dynamic testing of soils for research and commercial purposes. The equipment can operate both RC and TS testing (e.g., Isenhower 1979, Lodde 1982, Ni 1987, Hwang 1997, and Darendeli 2001). The equipment is the fixed-free type, where the soil specimen is fixed in place at the bottom and the driving force is applied at the top. The general principle employed in the RC test is to excite the soil specimen with a steady-state torsional motion over a range of frequencies to identify the first mode resonant frequency. The shear modulus can then be evaluated utilizing the well-defined boundary conditions and the specimen geometry and mass. Material damping is determined by the half power bandwidth or free vibration decay method. The difference between the TS test and the RC test is mainly in the excitation frequency. In the TS test, a slow cyclic loading in the range of 0.01 to 10 Hz is applied to the specimen. In this project, the TS test was performed at a frequency of 0.5 Hz. Shear modulus and damping were determined based on the characteristic of the hysteresis loop. The drive system and equipment damping for this apparatus were calibrated

according to Sasanakul and Bay (2008, 2010). In the RC test, the first mode resonant frequency is used for the analysis. For this study, the resonant frequency ranged from 10 to 150 Hz for soil samples and 400 to 600 Hz for rock samples.

It is extremely important to handle undisturbed soil samples with care as sample disturbance can have a significant effect on testing results. Each soil sample was carefully cut from the tube. First, each end of the selected portion of the tube was cut using a tube cutter. Next, the side of each tube was cut vertically using a band saw. In most cases, the tube springs opened after cutting, and the soil sample was removed. When the tube did not spring open, the opposite side of the tube was cut to remove soil with minimal disturbance. In addition to the undisturbed soil samples, three additional sand samples taken from the Shelby tube samples were prepared by reconstitution. The sample preparation was conducted by dry pluviation in layers to achieve the field unit weight estimated based on weight and volume relationships of soil in a given section of the Shelby tube sample. Due to a limited number of Shelby tube samples, soil samples from the core sampler were also used for RC and TS testing. Soil specimens were carefully hand-trimmed to a diameter of approximately 1.4 inches and a height of about 3.0 inches using a trimming device and wire saw. Water content and index properties were determined using the trimmings.

Intact rock samples were carefully selected from the core samples. Specific gravity of each rock specimen was measured according to ASTM C127-88 and AASHTO T85-91 prior to testing. The rock sample preparation method is similar to Tuff (i.e., igneous rock sample) preparation done by Jeon (2008). For this study, the typical diameter of the specimens was approximately 2.4 inches and the sample was not re-cored. Each specimen was cut to a specified length in order to achieve the diameter to length ratio of approximately 1:2. The top and bottom of each specimen was trimmed using rotary grinding and sandpaper to create a smooth and flat surface. The specimen was attached to the top and bottom pedestals of the testing device using epoxy glue that was allowed to cure for approximately 24 to 48 hours. Due to the torque limitation of the equipment, only the RC test was performed on the rock specimens.

In this study, each soil specimen was tested with at least three confining pressures of $0.5\sigma'_{mo}$, σ'_{mo}, and $2\sigma'_{mo}$, where σ'_{mo} is the mean in-situ confining stress. Due to the maximum safe confining pressure achievable in the laboratory of approximately 150 psi, the maximum confining pressures for deep samples were at σ'_{mo} and the other two confining pressures were at $0.5\sigma'_{mo}$ and $0.25\sigma'_{mo}$. Each rock sample was tested with no confinement and at least two additional confinements of $0.25\sigma'_{mo}$, $0.5\sigma'_{mo}$, and/or σ'_{mo}. It was noted that effect of confinement on dynamic properties of rock was minimal as discussed in Sections 4.4.2 and 4.4.3.

4. Results and Analysis

This project generated a large set of data from a field and laboratory investigation of two sites in the South Carolina Coastal Plain. All of the data and detailed analysis can be found in the appendices. This chapter summarizes key findings and observations from the field and laboratory investigation that are useful for engineering design and future SCDOT studies.

4.1. General Observation of Geotechnical Borehole Drilling

For Site A, three boreholes were drilled during a 19-day period, from 1/18/2017 to 2/5/2017. The original plan was to drill to a target depth of 515 ft. The presence of thick sand layers, particularly at depths below 272 ft, caused drilling difficulties during when completing the first borehole. In addition, a significant amount of borehole fluid circulation was lost when advancing below 505 ft and as a result, the borehole became unstable and had to be terminated at 505 ft, 10 feet from the target borehole depth. The P-S logging was only performed between the depths of 300 and 470 ft while the drilling casing/core rod was left in place at the upper 300 ft to maintain the open borehole in the unstable thick sand layers. The FWS logging was not performed at this site due to the instability of the borehole. To allow additional data collection, two additional boreholes were drilled at this site. A second borehole was successfully drilled to the same 505 ft depth as the first borehole utilizing PVC casing to stabilize the hole which allowed additional P-S logging to be performed from the surface to a depth of 300 ft. The P-S logging data of the second borehole was analyzed and combined with the data from the first borehole. The third borehole was drilled to a depth of 300 ft and data from the first borehole was used to select additional Shelby tube sample locations in soil zones.

For Site B, two boreholes were drilled during a 32-day period, from 2/6/2017 to 3/9/2017. The first borehole was drilled to the target depth of 615 ft as planned. The P-S logging and FWS logging were performed at this borehole to a depth of 600 ft. A second borehole was drilled to a depth of 150 ft and data from the first borehole was used to select Shelby tube sample locations in soil zones.

4.2. Geotechnical and Geological Description of Soil Profiles

Results from geotechnical and geological logging are summarized in Fig. 4.1 for Site A and Fig. 4.2 for Site B. An overview description of each soil profile is presented below.

Site A consisted of soil deposits from Quaternary and Cretaceous periods. Younger material from Quaternary deposits, located in the top 53 ft, are Penholoway alloformation. Because this formation has not been used since the early 1980, it is considered informally as an alloformation (Doar 2018). The deposits consisted of silty and clayey sands interbedded with a relatively thin layer of low plasticity clay and silt. Cretaceous deposits consist of Peedee formation located between 53-196 ft and Black Creek group formation and possible Donoho Creek, Bladen, and Coachman formations located below 196 ft. The deposits were composed of a variety of materials, with clayey sand and silt layers appearing to be dominant. These layers were interbedded with layers of low to high plasticity clay and silt with thicknesses ranging from 1 to 2 ft. Relatively thin

rock layers consisting mainly of sandstone or calcareous sand with thicknesses of less than 3 ft were intermittently observed within these layers. Approximately 16-26 ft thick sandstone and limestone layers interbedded with thin clayey sand layers were found at depths between 300-345 ft, and additional sandstone/limestone layers at depths of 450-460 ft. As discussed previously, drilling difficulties were encountered because of sand layers at depths below 272 ft. Below these unstable layers, at depths between 387-461 ft, silty and clayey soils with wide range of plasticity were observed. These layers were underlain by relatively thick silty and clayey sand layers which again caused drilling difficulties. These sands were very fine to medium loose.

Site B consisted of Quaternary, Tertiary and Cretaceous periods. Quaternary deposits located in the top 11 ft are Ten Mile Hill formation. The deposits consist of silty and clayey sand. Below the Quaternary deposits are Tertiary and Cretaceous deposits. The boundary between Tertiary and Cretaceous occurred at a depth of 228 ft below the ground surface. There were two formations including Williamsburg and Rhems formations in the Tertiary section. The shelly limestone layers were found at a depth between 19-48 ft. The soil layers directly below the limestone/sandstone at 43-262 ft were mainly sandy soils with weak to strong cementation. Two additional layers of limestone/sandstone at depths of 115 and 197 ft were observed in the Tertiary deposit interbedded with layers of low and high plastic clayey and silty soils. The level of cementation of these materials was highly variable. At a depth of 230 ft, the Cretaceous deposits from Peedee, Donoho Creek, and Bladen formations consisted of mostly cemented clayey and silty soils interbedded with layers of sand. The thickest sand layer was greater than 30 ft thick and found at a depth of 508 ft. Shell fragments were also observed within these sand layers.

Based on the visual observation and geological classification for both sites, a layer of competent rock was not encountered at the depths investigated.

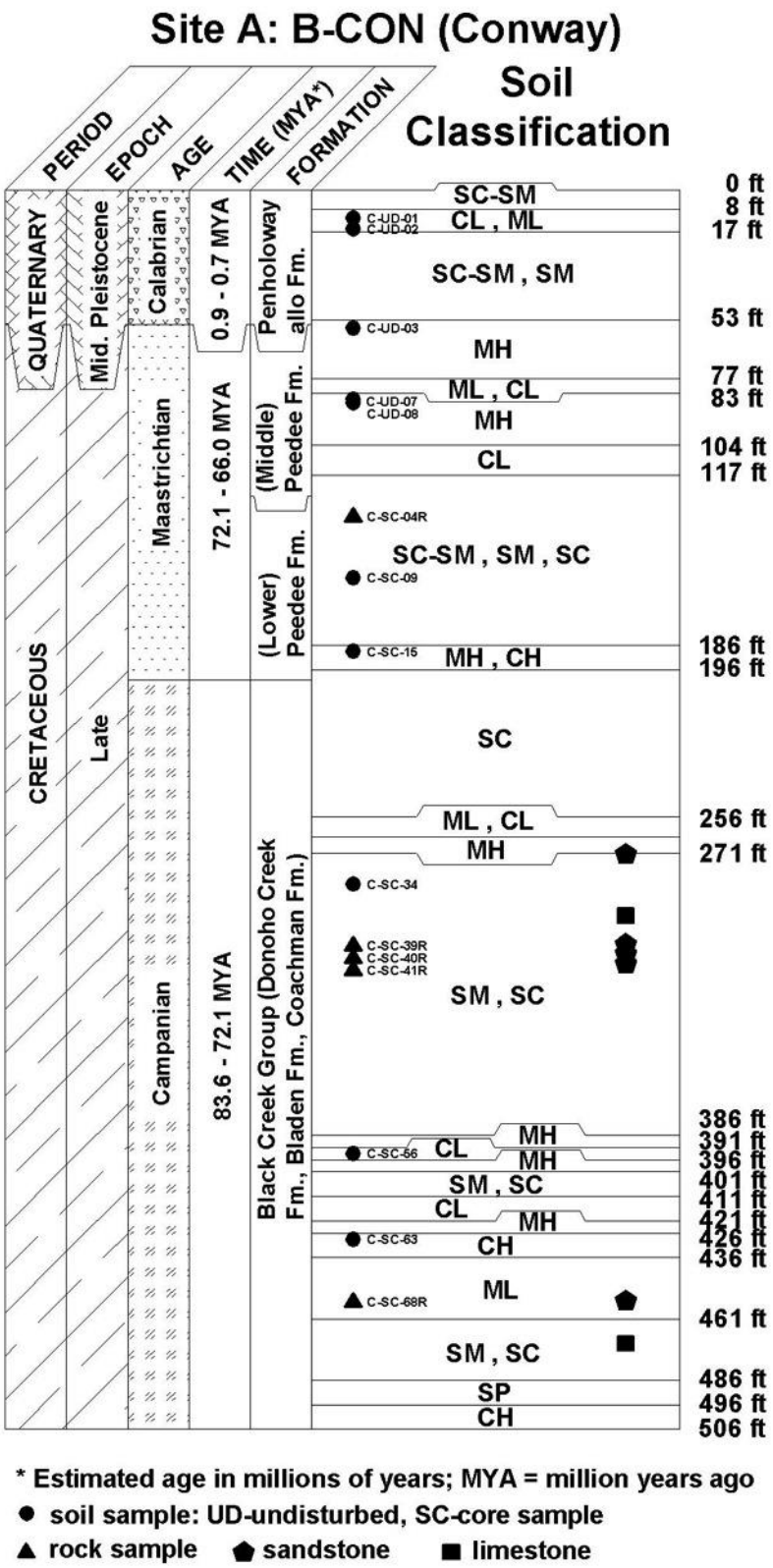

Figure 4.1 Soil Classification and Geological Information for Site A

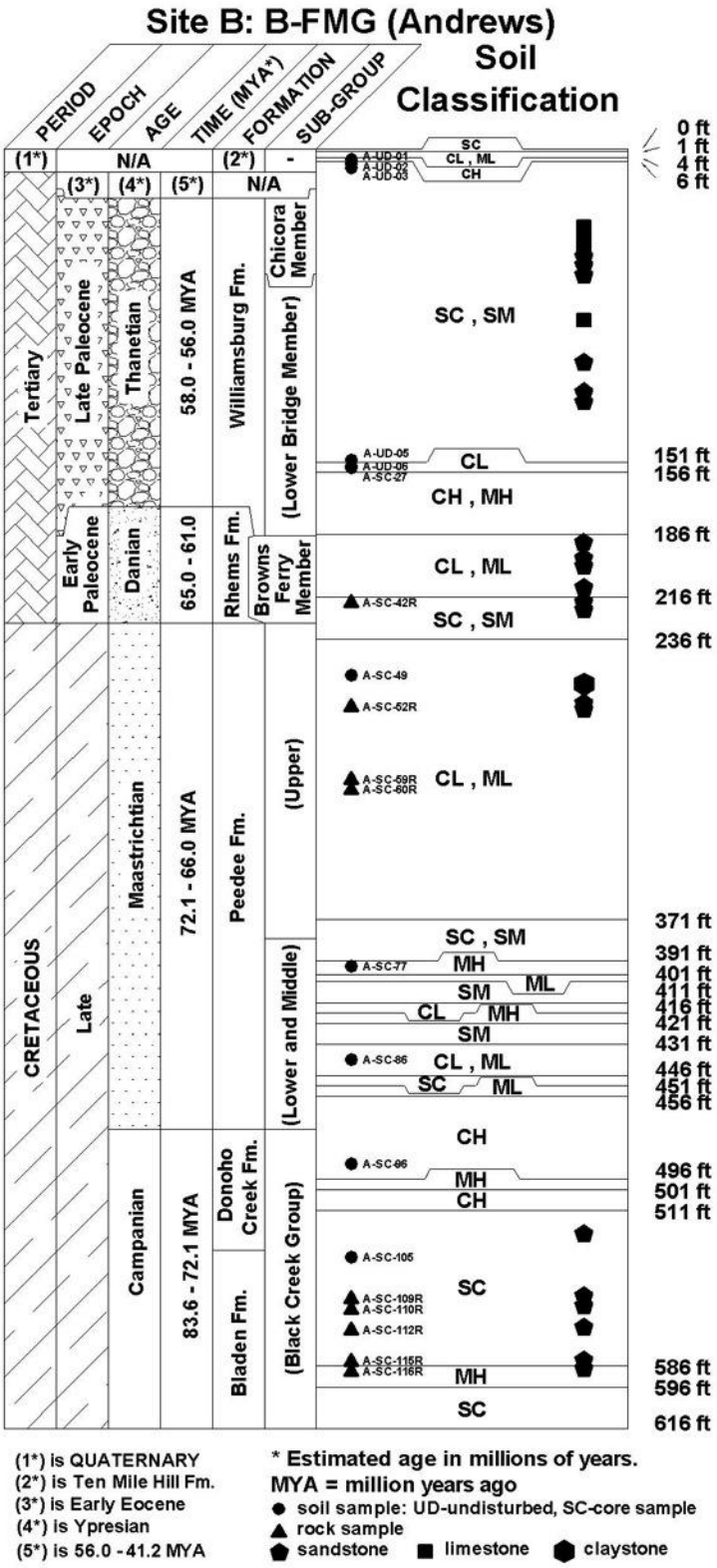

Figure 4.2 Soil Classification and Geological Information for Site B

4.3. Field Measurements of Shear Wave Velocity Profiles

In this study, the V_s profiles were obtained from the borehole P-S suspension logging, FWS logging, combined MASW-SASW, and combined MASW-MAM methods. As described previously, the P-S logging was performed from the ground surface to a depth near the bottom of the boreholes. The FWS logging was performed in a similar manner to the P-S logging but could only be completed at Site B. Thus, the borehole methods provided Vs profiles to a depth of 470 ft for Site A and a depth of 600 ft for Site B. The MASW-SASW tests generated V_s profiles down to a depth of approximately 220 ft for both sites. The combined MASW-MAM generated profiles down to depths of 4921 ft for Site A and 2625 ft for Site B. This method can generate deeper profiles than other surface wave methods because unlike the typical MASW and SASW which use an active energy source, the MAM method uses passive ambient noise as the wave source and a large array spacing (over 3000 ft) as described previously. This method can produce experimental dispersion curves over a wide frequency range (longer wavelength) resulting in very deep V_s profile models. More detailed analyses of the MASW-MAM method for this study can be found in section 4.3.1 and Appendix B.

4.3.1. Summary of Surface Wave Data Analyses

This section includes a summary of surface wave data analyses from the combined MASW-SASW and MASW-MAM methods. Both methods are not commonly performed in SC. In fact, the MASW-MAM method was used for the first time in this study to characterize a deep V_s profile. It is important to understand that these surface wave methods are not direct measurements of shear wave velocity and the results rely heavily on knowledge and experience of the data analyst. The data analyses presented in this section were conducted by experts in the field and approaches require expert analysis and experience and therefore are not used as part of routine wave velocity profile collection. More detailed information can be found in Appendices A and B.

4.3.1.1. MASW-SASW Data Analysis and Results

As mentioned in Section 3.2.4, both MASW and SASW methods generate dispersion curves. These curves were combined as shown in Fig. 4.3(a) and Fig. 4.4(a) for Site A and Site B, respectively. For Site A, there appears to be two phase velocity trends in the data: a higher velocity trend that appears dominant over a wide frequency range (longer wavelength) and a lower velocity trend that occurs over a narrower frequency range (shorter wavelength). For Site B, the Rayleigh wave propagation is very complex with dominant higher mode Rayleigh wave energy at frequencies between 10 and 20 to 25 Hz and no evidence of the fundamental mode Rayleigh wave over this frequency range. This type of dispersion curve signature indicates that there is a shallow high velocity layer at the site.

For Site A, the representative dispersion curve shown in Fig. 4.3(a) was modeled using inverse modeling with the effective modeling solution in the software Seisimager to develop several V_s models corresponding to different receiver spacing. An example of a selected V_s model for Site A

is shown in Fig. 4.3(b). The effective mode solution was necessary for inverse modeling the dominant higher mode Rayleigh wave energy at high frequencies associated with a higher velocity (stiff) surface layer and a smooth transition from the fundamental to the first higher mode at low frequencies associated with an abrupt increase in V_s at depth. The V_s models developed from effective mode inversion of the Rayleigh wave dispersion curves corresponding to 246 ft (75 m) SASW receiver spacing is recommended by GeoVision (see Appendix A), as it is the most representative of the average V_s profile for Site A as shown in Fig. 4.3(b).

For Site B, the representative dispersion curve shown in in Fig. 4.4(a) was modeled using the forward modeling with a multi-mode solution (mode with highest relative energy) in the software Seismager, and effective mode modeling solution (3D global solution) in the software WinSASW V3 to develop the V_s models shown in Fig. 4.4(b). The shallow high velocity layer presented at this site was modeled with variable V_s and thickness. The best representative V_s profile was selected based on the best fit data at the higher mode energy between 10 to 15 Hz. Two profiles generated from the multi-mode model and the effective mode model were very close with a difference of 6% for the average V_s at the top 100 ft as shown in Fig. 4.4(b).

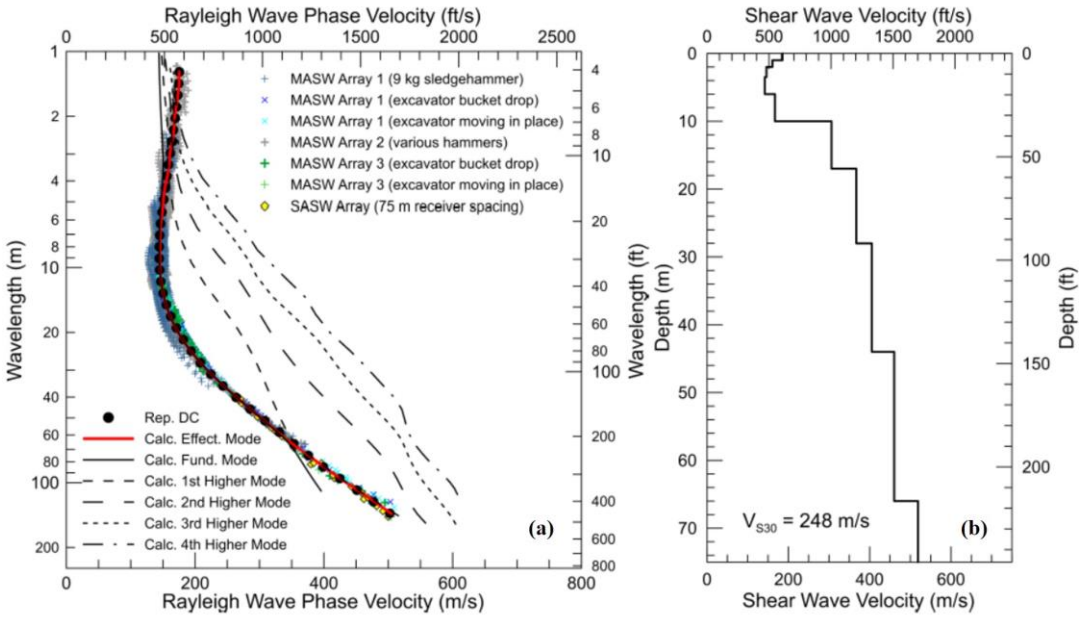

Figure 4.3 Inversion Results for Site A from MASW-SASW Method: (a) Dispersion Curves, and (b) Selected V_s Model

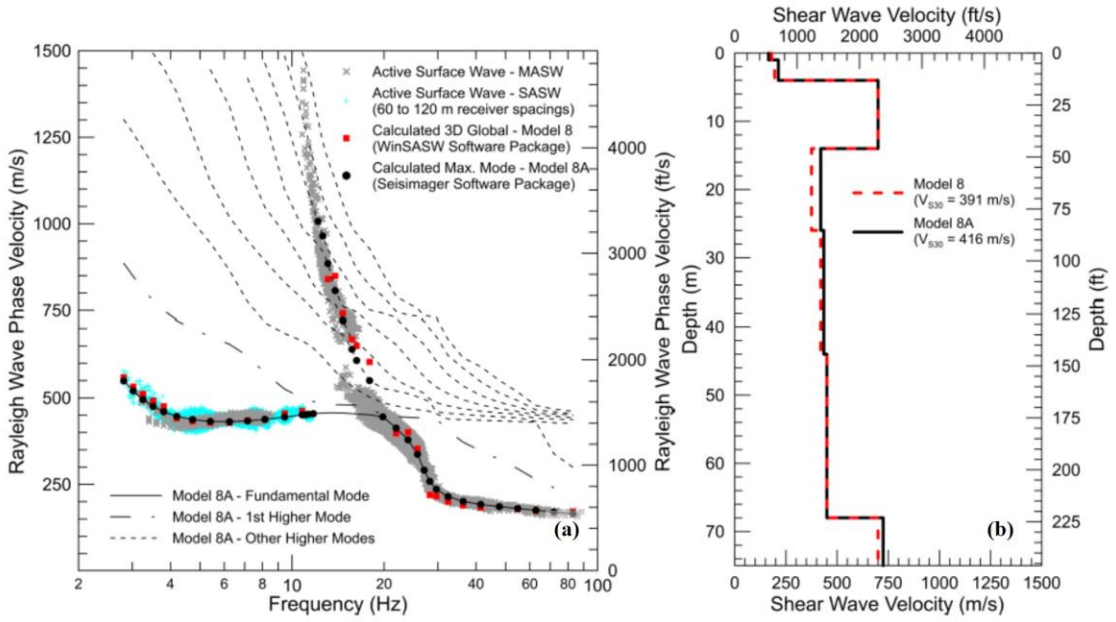

Figure 4.4 Inversion Results for Site B from MASW-SASW Method: (a) Dispersion Curves, and (b) Selected V_s Models

4.3.1.2. MASW-MAM Data Analyses and Results

In addition to the dispersion curves shown in Figs. 4.5(a) and 4.6(a), the horizontal to vertical (H/V) spectral ratio curves were generated by the combined MASW-MAM method (see Section 3.2.5) for Site A and Site B as shown in Fig. 4.5(b) and Fig. 4.6(b), respectively. The H/V curves represents the fundamental site frequency and based on Figs 4.5(b) and 4.6(b) a consistency of low-frequency peak is shown suggesting that the fundamental site frequency is relatively uniform across the footprint of the MAM arrays. Typically, the frequency corresponding to a well-defined peak can be used to estimate the fundamental shear wave resonant frequency of the site and/or the lowest-frequency peak of the fundamental mode Rayleigh wave ellipticity (Lermo and Chavez-Garcia 1993, Lachet and Bard 1994, SESAME 2004). However, there were a few other peaks observed and these peaks are believed to be indicative of shallow velocity impedance contrasts. When a more moderate impedance contrast is present, the frequency corresponding to the peak may be more representative of the fundamental site frequency (Bonnefoy 2004). The higher frequency peak is visually variable in its peak location, width, and amplitude across the extent of the arrays. This indicates that the depth and stiffness of a shallow velocity contrast is spatially variable across the sites.

The inversion process was performed as described in Section 3.2.5. The median V_s profiles obtained from each site are shown in Figs. 4.5(c) and (d) for Site A and Figs. 4.6(c) and (d) for Site B. The median V_s profile obtained from an inversion parameterization of 2.0a was recommended by the UT Austin (see Appendix B) to be a representative V_s profile for each site.

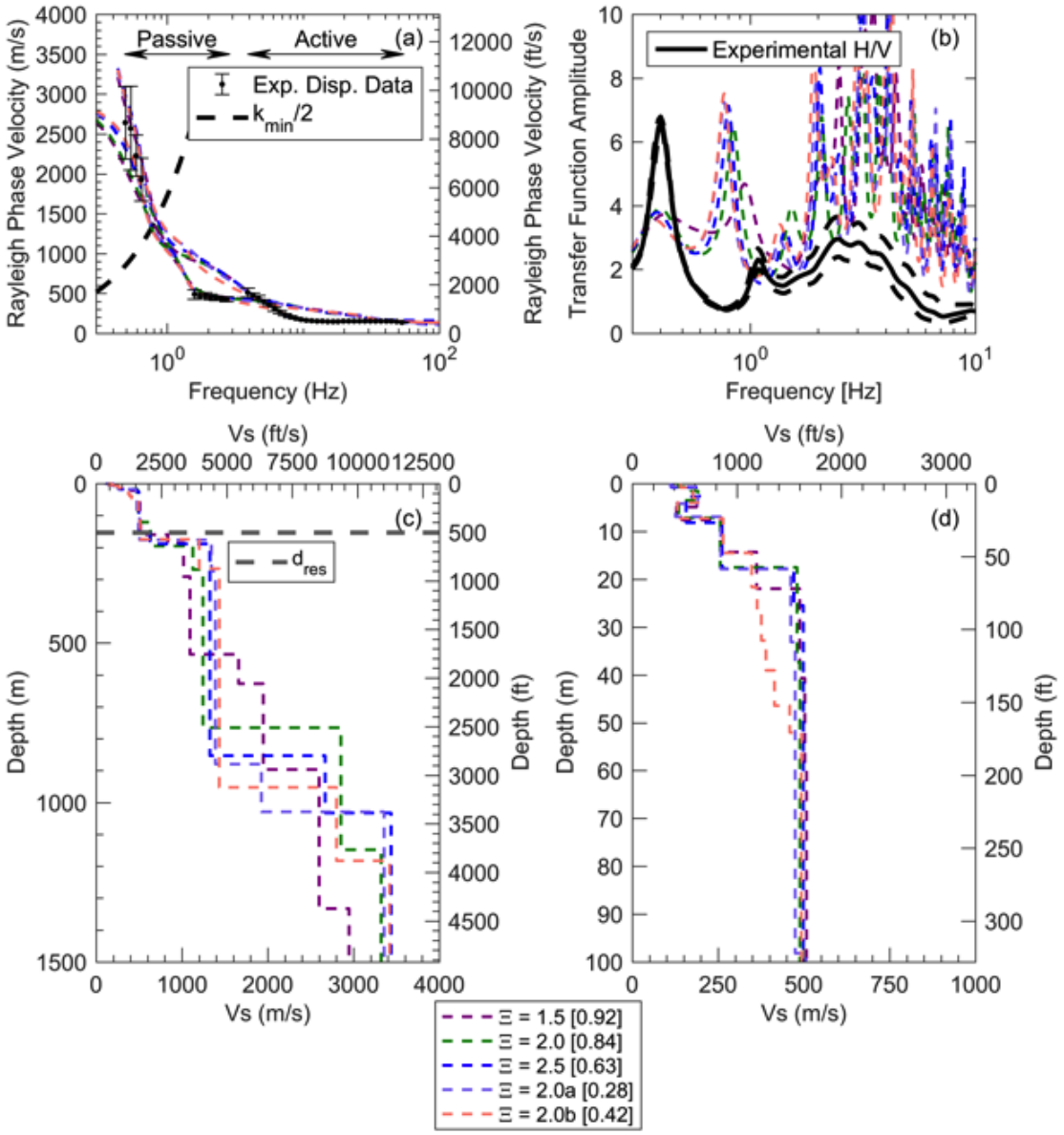

Figure 4.5 Median Inversion Results for Site A from MASW-MAM Method Shown for Each Inversion Parameterization (i.e., layering ratios Ξ = 1.5, 2.0, 2.5, 2.0a, and 2.0b): (a) Dispersion Curves, (b) H/V Curves, (c) V_s Profiles Shown to a Depth of 4900 ft, and (d) V_s Profiles Shown to a Depth of 328 ft

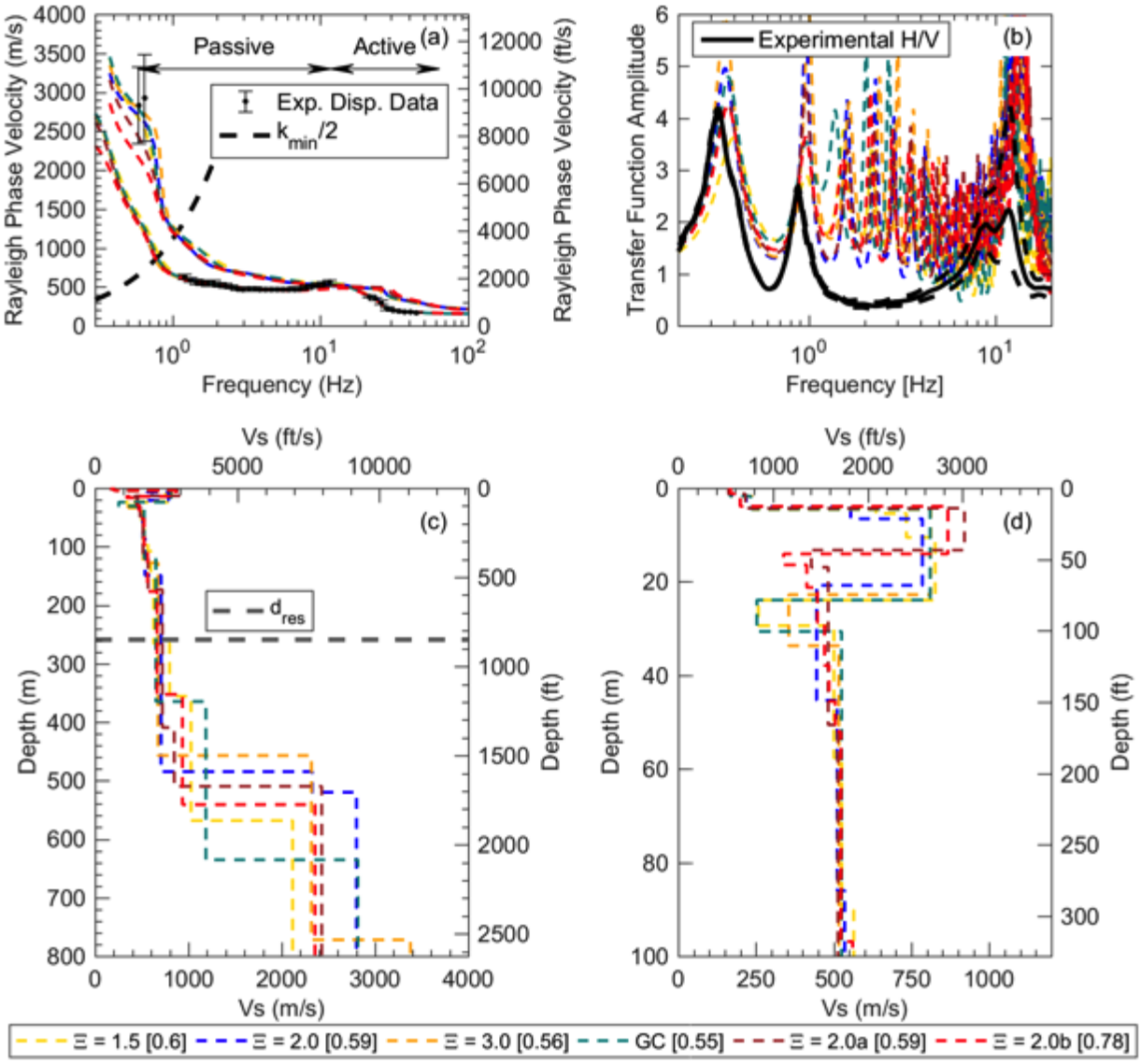

Figure 4.6 Median Inversion Results for Site B from MASW-MAM Method Shown for Each Inversion Parameterization: (a) Dispersion Curves, (b) H/V Curves, (c) V_s Profiles Shown to a Depth of 2625 ft, and (d) V_s profiles Shown to a Depth of 328 ft

4.3.2. Comparison of V_s Profiles for Site A

Fig. 4.7 presents the V_s profiles found from P-S logging, MASW-MAM and MASW-SASW methods for Site A. For comparison purposes, profiles are shown to depths of 800 ft and 300 ft in Fig. 4.7(a) and 4.7(b), respectively. These depths are chosen to provide overall observation of the B-C boundary provided by the MASW-MAM method and allow more detailed comparisons between different geophysical methods at shallower depths. It was noted that several V_s profiles were generated from both surface geophysical methods during the inversion process of the data analyses as mentioned in Section 4.3.1. The profiles were selected based on the subcontractors'

recommendations based on data quality, boring logs, and geological information at the site. Additional V_s profiles and more detailed data analysis and interpretation can be found in Appendices A, B, and C. The P-S logging method measured the V_s profile with a resolution of 1.5 ft, therefore soil layers with thickness greater than 1.5 ft and the variation of V_s in very stiff and/or cemented soil layers as well as rock layers are captured by the P-S logging method.

For Site A, approximately seven to ten different layers were obtained from the MASW-SASW and the combined MASW-MAM methods based on the surface wave data interpretation. The V_s generally increased as the depth increases. For both methods, the V_s ranged from 490-985 ft/s for the Quaternary deposit (Penholoway alloformation) and from 985-1640 ft/s for the Cretaceous deposit (Peedee, Donoho Creek, Bladen, and Coachman formations) below 53 ft. There was no clear separation indicating difference in the V_s profile for each formation. Some discrepancies between the borehole and surface geophysical methods were observed; however, in general, the V_s for the younger Quaternary deposits were lower than the older Cretaceous deposits. The lower values of V_s were likely related to the lower confinement at the shallower depths.

At depths between 374-482 ft, the V_s ranged from approximately 2,600 to 3,280 ft/s and the core samples from these layers were described visually in the geologic log as alternating layers of loose and hard beds caused by carbonate cementation. These materials are calcareous clayey sand with strong reaction with hydrogen chloride (HCl). There were some trace of shell fragments and muscovite throughout the core. The USCS classifications of these materials are SC and SM.

At depths between 150-295 ft, similar calcareous clayey or silty sand was also found, but the core samples were relatively loose and more friable. The reaction to HCl was weak to moderate indicating less carbonate cementation. This observation is consistent with the lower V_s values measured for this material, ranging from 1312-1967 ft/s. There were a few thin layers of strong carbonate cemented sand that are consistent with the spikes in the V_s profile within these depths.

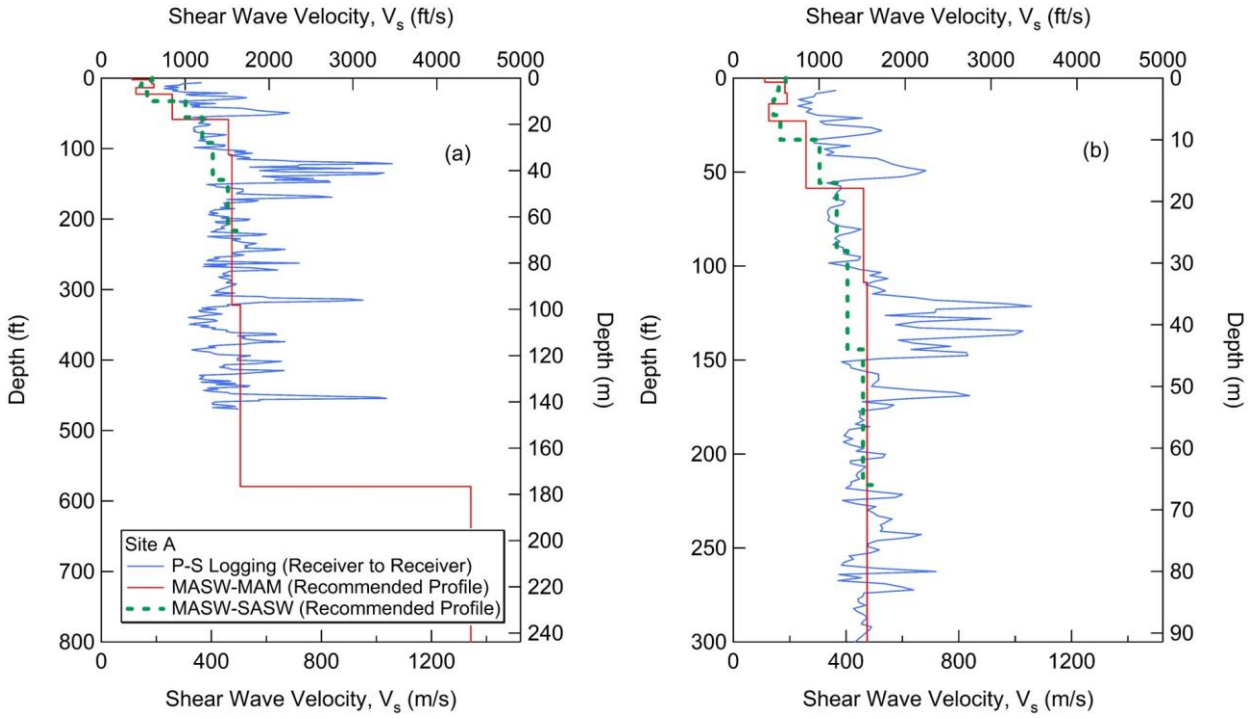

Figure 4.7 V_s Profiles for Site A: (a) Shown to a Depth of 800 ft, and (b) Shown to a Depth of 300 ft

At depths between 296-505 ft, two sharp spikes for V_s of 2953-3280 ft/s at a depth of 315 ft and 456 ft were consistent with sandstone samples described as shelly sandstone. This material appeared to be phosphatic grains tightly cemented with carbonate and had very strong reaction with HCl. Drilling difficulties were encountered at this depth range (300-505 ft) and half of the attempts to collect core samples failed. In addition to the shelly sandstone, the collected samples were mostly classified as loose fine to medium sand with a small percentage of clay, and reaction to HCl was none to weak. These materials were interbedded with a few thin layers of low to high plasticity clay and silt, cemented clay, and sandstone. The V_s values, with the exception of the sandstone layer, are between 1050-2165 ft/s. The lower V_s values are consistent with loose, relatively weak cemented sands and the higher values were consistent with cemented clay. Photographs of calcareous sand/sandstone from Site A are shown in Fig. 4.9. Even though the V_s values for these materials are over 2300 ft/s, they were only found sporadically throughout the borehole depth. As a result, the top of soft rock layer with consistent V_s of 2300 ft/s or higher was not reached and was located at a deeper depth. The MASW-MAM method suggests that the stiff layer with a very high V_s of over 4000 ft/s may be located at a depth below 580 ft.

A comparison between SPT N-values and V_s in the top 120 ft is shown in Fig. 4.8. The SPT-N values with depth are plotted in Fig. 4.8(a) and the V_s profiles found from the P-S, MASW-MAM and MASW-SASW methods are plotted with depth in Fig. 4.8(b). In addition, the V_s values found using the V_s-SPT correlations of Andrus et al. (2009) for sand and Seed and Idriss (1981) for all soils are plotted in Fig. 4.8(b). The results found using the Andrus et al. (2009) and Seed and

Idriss (1981) correlations matched reasonably well with the results from MASW-SASW and MASW-MAM methods at shallow depths (<30 ft) (the Andrus et al. (2009) correlation has a better match). The V_s profiles from the SPT correlation using Andrus et al. (2009) approach are lower than Seed and Idriss (1981) approach, particularly at deeper depths. The top 50 ft of the V_s profile from the P-S logging method was much higher than other methods.

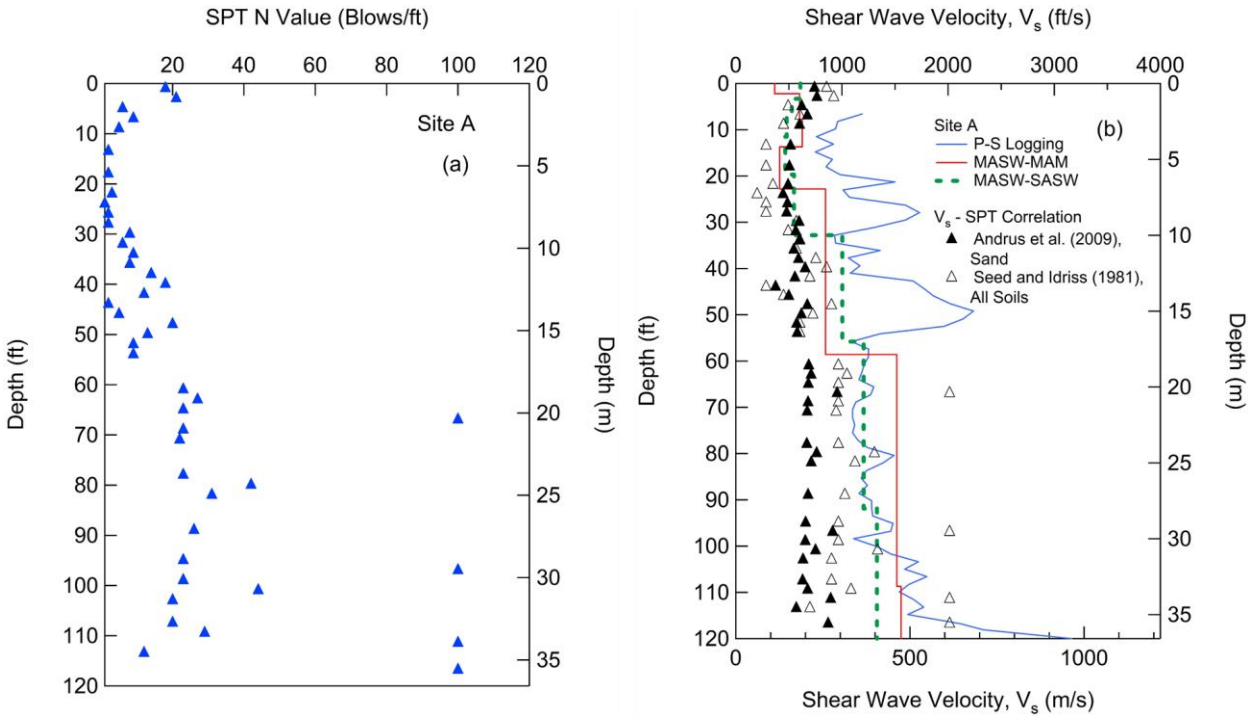

Figure 4.8 (a) Variation of SPT N Value with Depth, and (b) Comparison between V_s Profiles between the V_s-SPT Correlation and Results from Geophysical Methods for Site A

The average V_s in the top 100 ft and 200 ft of the profile obtained from the three different testing methods are presented in Table 4.1. Results from the P-S logging show higher average values of V_s than that of the other two methods resulting in a different NEHRP site class. There are a few possible explanations for this discrepancy. The surface methods (MASW-SASW and MASW-MAM methods) characterize the average V_s based on wave propagation characteristics through a large volume of soil/rock and the profiles typically consist of a limited number of representative layers. Conversely, the P-S logging method can be used to characterize the average V_s of the localized soil/rock properties within the tested borehole, thus the profiles provide high level of details with higher resolution. It is possible that the depth and stiffness of cemented or soft rock layers is spatially variable across the site causing a large discrepancy between local and global V_s profiles. The other explanation could be related the problem with borehole drilling at Site A. The P-S logging data at depth below 300 ft was obtained from the uncased borehole. While the P-S logging data at the top 300 ft was obtained from the offset cased hole about approximately 1 month

after the first set of data was collected. The actual reason remains unknown but it is also important to note that the average V_s for the P-S logging method did not include data from the top 6 ft. In addition, Table 4.1 shows that the B-C boundary was not reached based on the V_s profiles from the P-S logging and SASW methods. The combined MASW-MAM provides a possible B-C boundary at a depth of 580 ft.

Table 4.1 Summary of Average Shear Wave Velocities and Possible B-C Boundary for Site A

Method	100 ft		200 ft		B-C Boundary (ft)
	Average V_s (ft/s)	NEHRP Site Class	Average V_s (ft/s)	NEHRP Site Class	
P-S logging	1225	C	1464	C	N/A
MASW-SASW	817	D	1039	D	N/A
MASW-MAM	860	D	1106	D	580

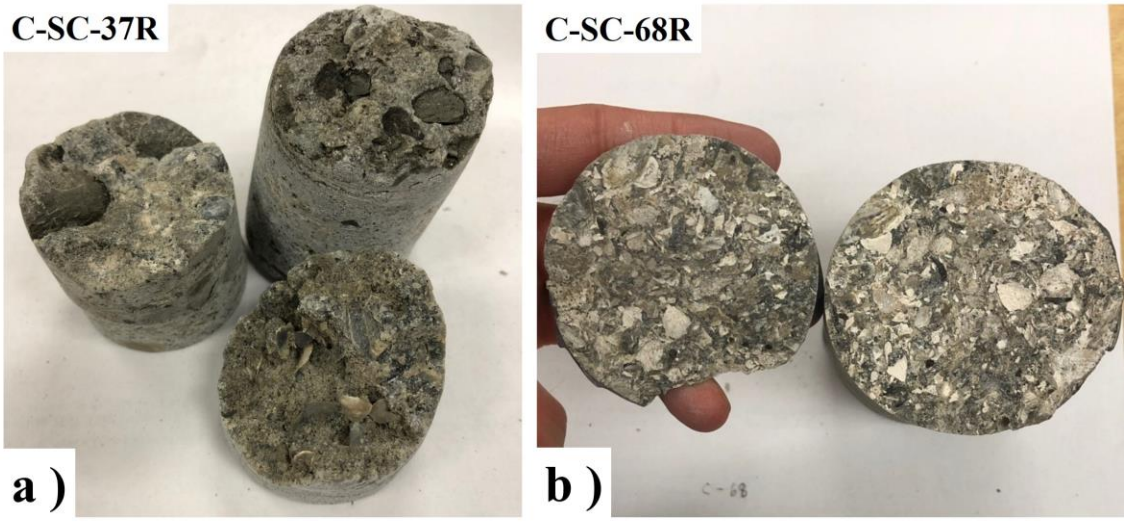

Figure 4.9 Calcareous Sand/Sandstone Samples from Site A at Depths: (a) 194-200 ft, and (b) 450-456 ft

4.3.3. Comparison of V_s Profiles for Site B

Fig. 4.10 presents the V_s profiles found from P-S logging, MASW-MAM, MASW-SASW, and FWS methods for Site B. For comparison purposes, profiles are shown to depths of 1800 ft and 300 ft in Fig. 4.10(a) and 4.10(b), respectively. For Site B, the MASW-SASW and the MASW-MAM methods suggested V_s profiles with six to eight layers of soil. The V_s slightly increased as the depth increased, with the exception of the layer between 13 to 43 ft. Overall, the V_s profiles from the MASW-SASW and MASW-MAM methods were similar, but the MASW-MAM provided slightly higher V_s values. The MASW-MAM method provided the V_s profile down to a

depth of 1343 ft; whereas, the MASW-SASW provided to a depth of 220 ft.

Similar to the results from Site A, the V_s profile obtained from the P-S logging method was more sensitive to layering than the two surface methods. The presence of limestone layers at shallow depths (20-43 ft) resulted in a V_s that is much higher (3280-5250 ft/s). Based on the visual classification, the limestone as shown in Fig. 4.11(a) was described as shelly limestone (biomicrite) with highly variable carbonate cementation. Some zones were well-indurated and cemented with a fine-grained carbonate cementation, other zones were friable where bivalves fragments occurred in a soft micritic (clay-size) matrix. The samples had high moldic porosity with the appearance of a shell hash (coquina), but most of the shells had either been replaced with calcite/micrite, or all of the shells had dissolved leaving a calcite-cemented clay matrix in its place. Even though the V_s values of the limestone layer were relatively high, the recovered core samples were not entirely intact and could not be used for resonant column and torsional shear testing.

Below the limestone layer (20-43 ft), layers of sand and calcite-cemented sandstone were observed at depths between 43-263 ft. These layers appeared to alternate based on the difficulty in recovering core samples and the spikes observed in the V_s profile as shown in Fig. 4.10 The sand was classified as SC. The V_s values for sand were approximately 984-1640 ft/s, while the V_s values for calcite-cemented sandstone were approximately 2297-3280 ft/s.

At a depth between 263-269 ft, calcareous sandstone layers were observed. These layers were underlain by low plasticity clay or sandy clay for depths between 263 to 364 ft. These thick clay layers were described as weakly to moderately cemented with carbonation or calcareous, sandy clay (mostly clay) with trace of shell fragments. This cemented clay had moderate to strong reaction with HCl. The clay layers were interbedded with claystone as shown in Fig. 4.11(b) and sandstone laminae. The V_s values for these layers ranged between 1772-2756 ft/s.

At a depth between 367-525 ft, the deposits were highly variable. A sharp spike was observed at the depth of 367 ft in the P-S logging data, with a V_s value of 4298 ft/s. The material observed at this depth was described as calcareous, clayey sand with strong reaction with HCl. Below this layer, at a depth of 387 ft, the V_s value was significantly lower and had a value of 984 ft/s. V_s increased to 2493 ft/s at the depth of 427 ft. The materials observed within these layers were described as laminated calcareous, silty clay as shown in Fig. 4.11(c). The core samples consist of dense clay interlaminated with very thin silty lenses. The material was friable (can break with hand) but firm. Below this layer, at a depth of 443 ft, a layer of calcareous sandy clay with strong cementation was found and had a V_s of approximately 2953 ft/s. Below this layer, the cementation appears to be weaker which was consistent with the lower V_s of 1476 ft/s from 466-508 ft. Another spike in V_s of over 3280 ft/s was observed at the depth of 525 ft and was attributed to the existence of a sandstone layer.

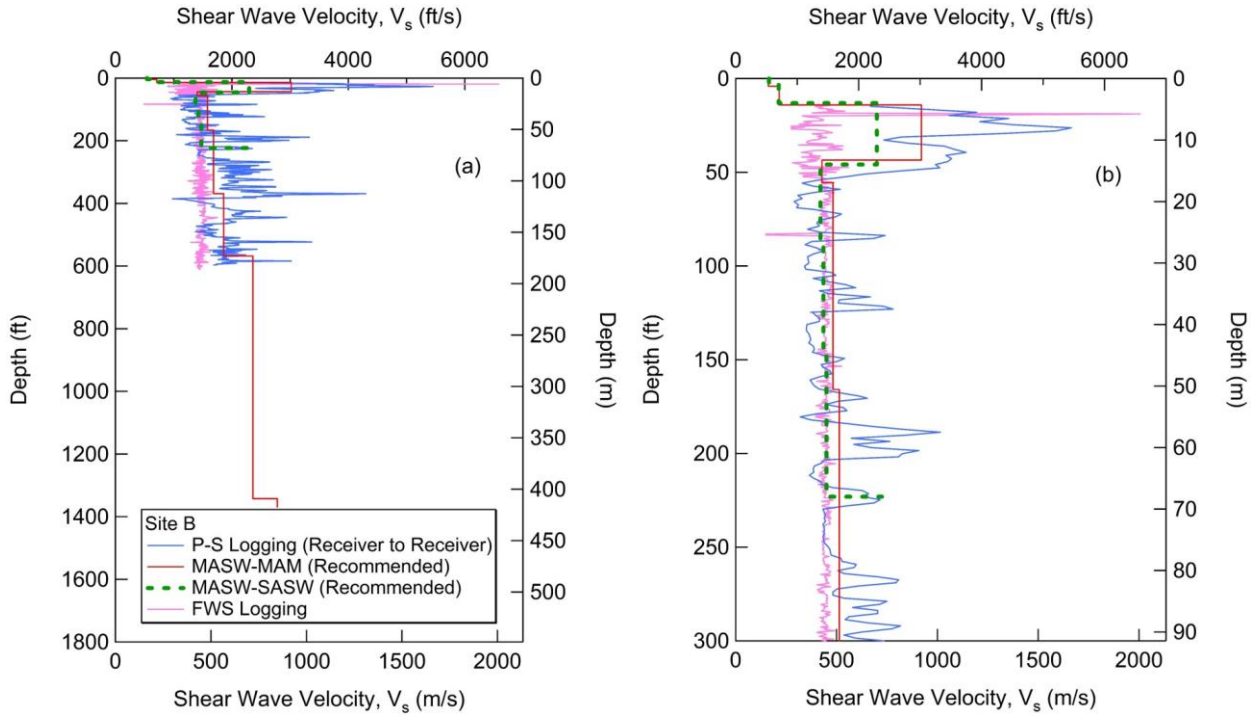

Figure 4.10 V_s Profiles for Site B: (a) Shown to a Depth of 1800 ft, and (b) Shown to a Depth of 300 ft.

At a depth between 526-615 ft, more calcareous sandy clay or clayey sand layers were found with the V_s ranging between 1640-2297 ft/s. These layers were underlain by approximately 13-16 ft of thick layers of sandstone as shown in Fig. 4.11(d), which were consistent with a V_s of 3028 ft/s. Near the bottom of the borehole, interlaminated/interbedded sand and clay was found. These materials had very little to no reaction with HCl, except where shell fragments occur, and the V_s was approximately 1640-1968 ft/s. Although the average V_s is 2034 ft/s between the depth 509-594 ft, based on the core logs and the V_s profile from the P-S suspension logging data, a consistent layer of rock with V_s over 2300 ft/s was not reached at the bottom of the borehole (615 ft). In comparison, results from the MASW-MAM method suggested that a layer with V_s of 2363 ft/s begins at a depth of approximately 568 ft.

The V_s profile obtained from the FWS logging method is also presented for comparison. Overall, the V_s values from FWS were lower than the other three methods and there was no variation of V_s with depth, with the exception of the results at approximately 18-19 ft depth where the limestone layers were observed.

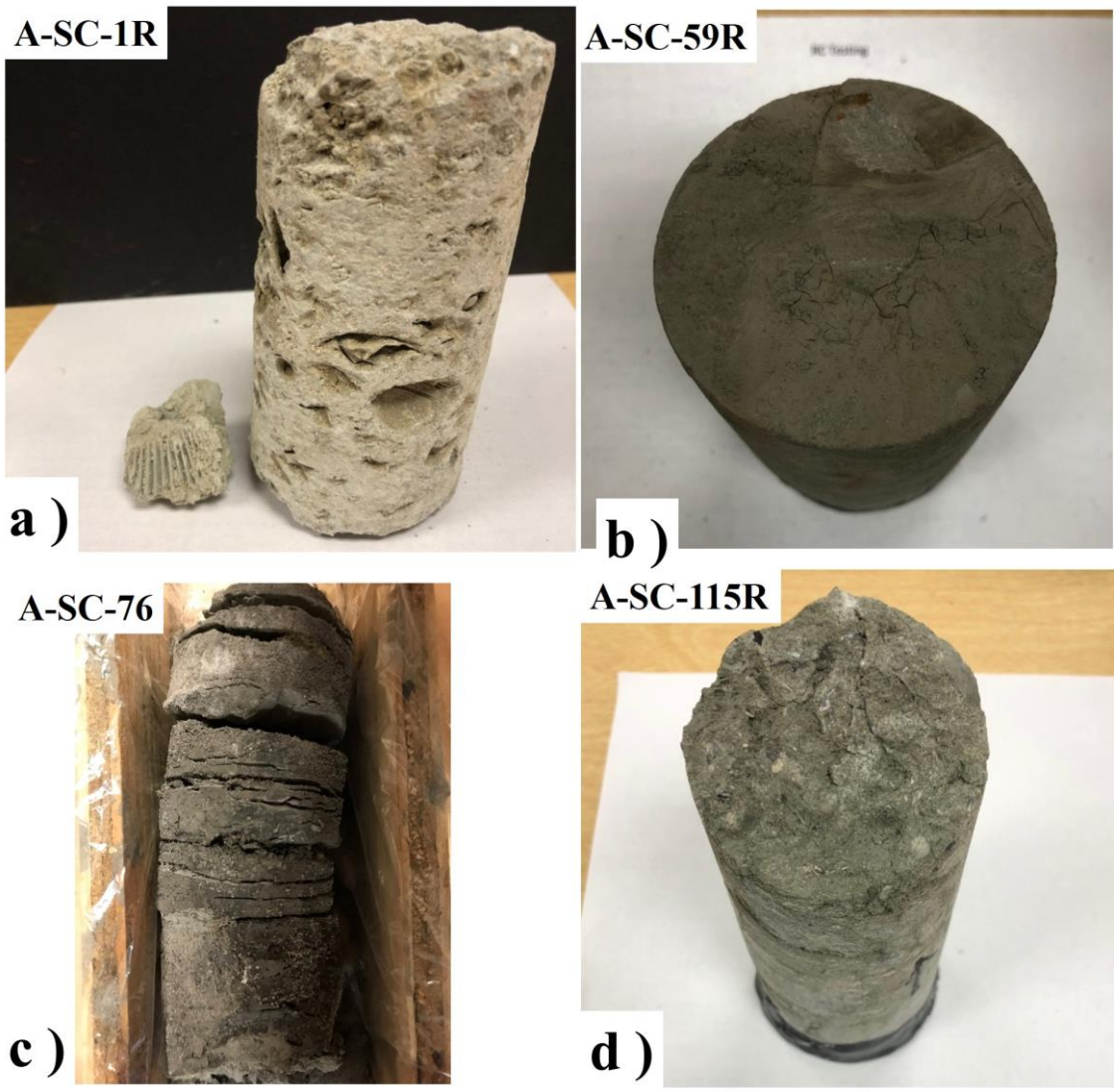

Figure 4.11 Samples from Site B: (a) Limestone from 23-26 ft, (b) Claystone from 300-305 ft, (c) Silty Clay from 394 ft, and (d) Sandstone from 580-584 ft

A plot of SPT N-values in the top 26 ft is shown in Fig. 4.12(a) and the corresponding V_s values obtained using the V_s-SPT correlations of Andrus et al. (2009) and Seed and Idriss (1981) are plotted in Fig. 4.12(b). The results of the P-S, MASW-MAM, MASW-SASW and FWS methods are also shown. Similar to Site A, the correlated results matched reasonably well with the results from MASW-SASW and MASW-MAM methods in the top 12 ft. P-S logging data is not available in the top 11 ft, therefore the results from the V_s-SPT correlations and surface wave methods are beneficial. Again, the V_s-SPT N-value correlation approach by Seed and Idriss (1981) shows a better match with results from the geophysical method at depths below 12 ft, however the SPT data is limited at this site because SPT testing was limited to soils above the limestone layer encountered at the depth of approximately 11 ft where the SPT blow count is above 100 blow/ft.

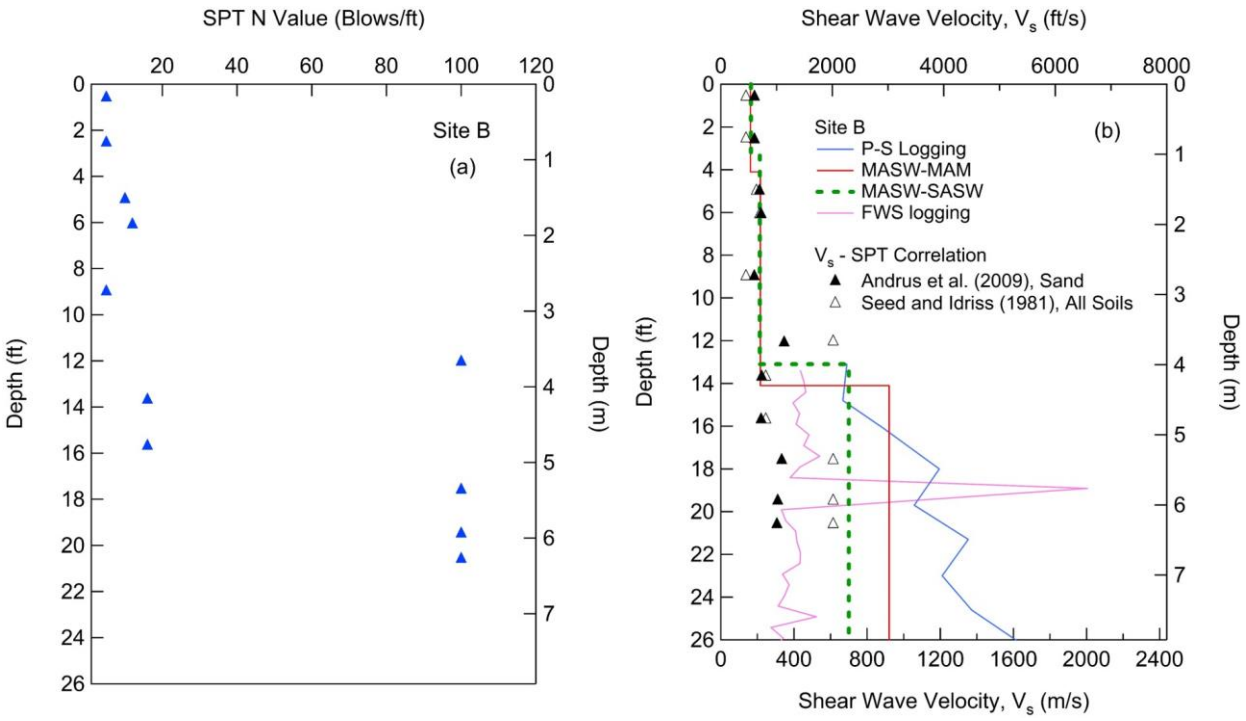

Figure 4.12 (a) Variation of SPT N Value with Depth, and (b) Comparison between V_s Profiles between the V_s-SPT Correlation and Results from Geophysical Methods for Site B

The average V_s in the top 100 ft and 200 ft of the profile obtained from different testing methods are presented in Table 4.2. Similar to Site A, results from the P-S logging shown higher average values of V_s than that of the other three methods, but all of the methods yielded the same site class. The combined MASW-MAM provided a possible B-C boundary at a depth of 1343 ft. Analysis of the MASW-MAM test method for Site B can be found in Section 4.3.1.2 and Appendix B. In general, the deeper V_s profile generated for the combined MASW-MAM method is a result of a dispersion curve that included a wider range of frequencies than other surface wave methods as was shown in Fig. 4.6.

Table 4.2 Summary of Average Shear Wave Velocities and Possible B-C Boundary for Site B

Method	100 ft		200 ft		B-C Boundary (ft)
	Average V_s (ft/s)	NEHRP Site Class	Average V_s (ft/s)	NEHRP Site Class	
P-S logging	1795	C	1650	C	N/A
FWS logging	1385	C	1429	C	N/A
MASW-SASW	1364	C	1408	C	N/A
MASW-MAM	1465	C	1536	C	1343

4.4. Laboratory Measurements of Dynamic Behaviors

A total of 35 soil and rock samples were tested to evaluate normalized shear modulus and damping curves for a wide range of strains. The effects of confinement, testing frequency, geological age, and plasticity index were examined. All of the soil samples were tested using both the RC and TS methods. The rock samples were tested using the RC method only. More detailed information and testing procedures can be found in Section 3.3 and Appendix F.

4.4.1. Dynamic Behaviors of Materials from Site A

RC and TS tests were performed on five samples from Shelby tubes and ten samples from the core sampler. The material properties and testing confinements are presented in Table 4.3. Soil samples were mostly clayey soils with a high plasticity index. Rock samples were classified as sandstone.

Table 4.3 Material Properties of Tested Samples for Site A

Sample ID[1]	Depth (ft)	σ'_{mo}[2] (psi)	Soil / Rock Type	%Finer	PI	ω_i[3] (%)	ω_f[4] (%)	Total Unit Weight (lb/ft^3)	σ'_m[5] (psi)
C-UD-01	11	5	CH	95.1	28	43.4	37.1	113	2, 5, 9
C-UD-02*	16	6	SC-SM	8.0	np[6]	0.0	0.0	95	6, 12, 23
C-UD-03	56	17	CH	91.6	44	35.3	37.1	116	9, 17, 35
C-UD-07	84	25	CH	87.0	43	40.7	35.8	112	13, 25, 51
C-UD-08	87	26	CH	93.8	47	42.6	37.7	113	13, 26, 52
C-SC-09	158	48	SC	30.6	14	20.3	26.4	116	24, 48, 96
C-SC-15	188	57	MH	70.2	19	31.2	28.3	116	29, 57, 114
C-SC-34	283	83	SC	43.6	15	30.1	27.0	109	41, 83, 124
C-SC-56	393	113	CH	95.7	34	36.5	36.1	109	26, 56, 113
C-SC-63	428	121	CH	80.0	39	43.5	40.5	109	61, 121, 147
C-SC-04R	133	45	Sandstone	-	-	-	-	157	0, 22, 45, 90
C-SC-39R	308	93	Sandstone	-	-	-	-	167	0, 46, 92
C-SC-40R	313	110	Sandstone	-	-	-	-	166	0, 55, 110
C-SC-41R	318	103	Sandstone	-	-	-	-	165	0, 52, 103
C-SC-68R	454	160	Sandstone	-	-	-	-	165	0, 80, 120

1. UD represents Shelby tube sample, and SC represents core sample; R is for rock sample

2. σ'_{mo} represents in-situ mean confining stress (K_0=0.5 assumed)

3. ω_i represents initial water content

4. ω_f represents final water content

5. σ'_m represents testing mean confining stress

6. np represents non-plastic

** reconstituted sample*

All of the results from RC and TS testing for soil samples are presented in terms of normalized modulus (G/G_{max}) and damping in Figs. 4.13 and 4.14, respectively. Both tests were carried out between strain levels of 10^{-5}% to 0.5% and when G/G_{max} values reached approximately 0.5. Similar results from the RC and TS testing were obtained for the G/G_{max} curves, but some differences were observed for the damping curves. These differences are due to the effects of

testing frequency discussed in the next section. The degradation of G/G_{max} curves occurs at strains 10^{-3} to 10^{-2}%. Damping values start to increase at strains higher than 10^{-2}%.

All of the results from RC testing for rock samples are presented in Fig. 4.15. The RC tests were performed up to G/G_{max} values of 0.9 when degradation was observed at slightly below 10^{-3}%. A slight effect of confinement was observed and is discussed in the next section.

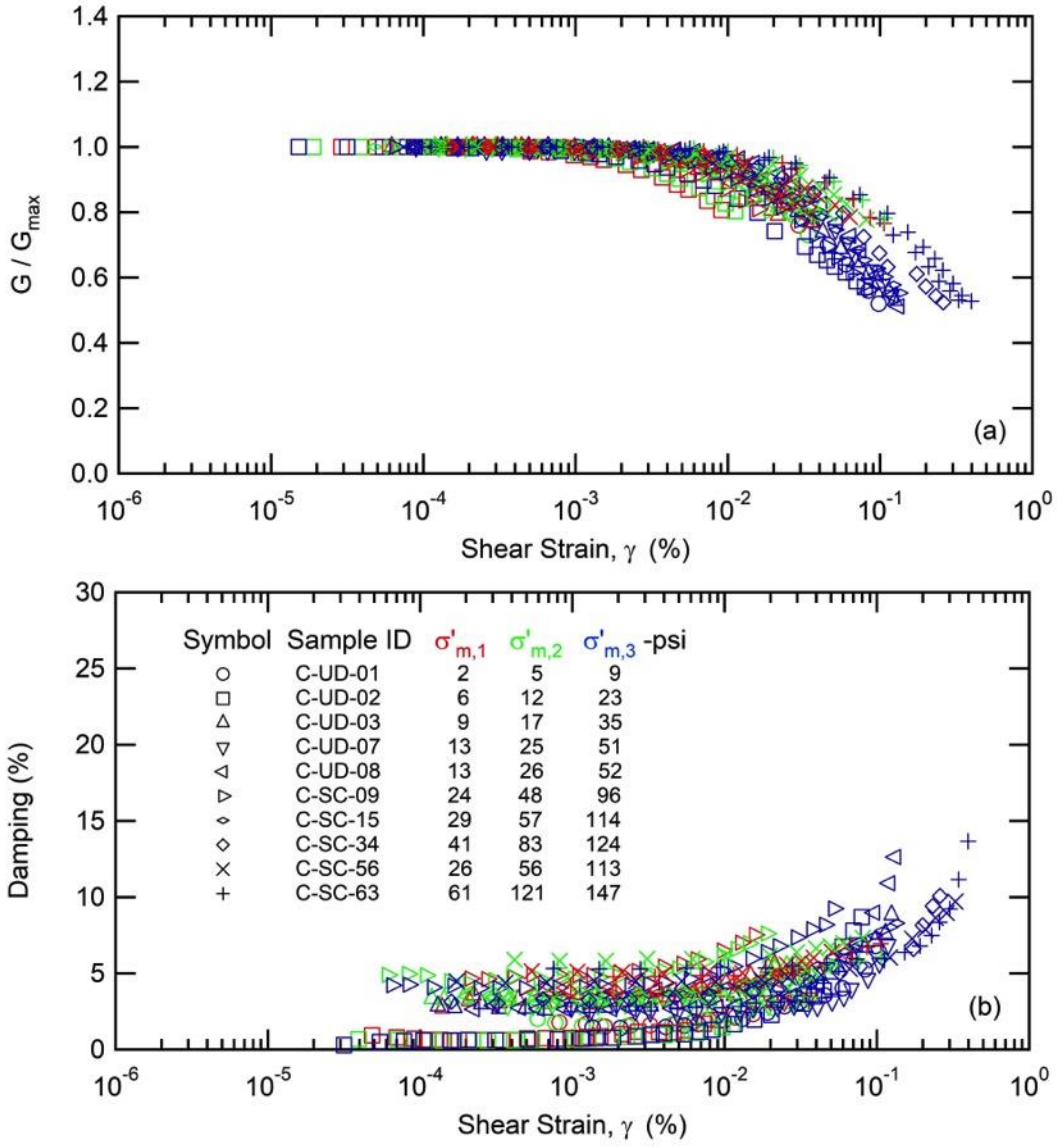

Figure 4.13 RC Testing Results for Soil Samples from Site A: (a) G/G_{max} Curves, and (b) Damping Curves

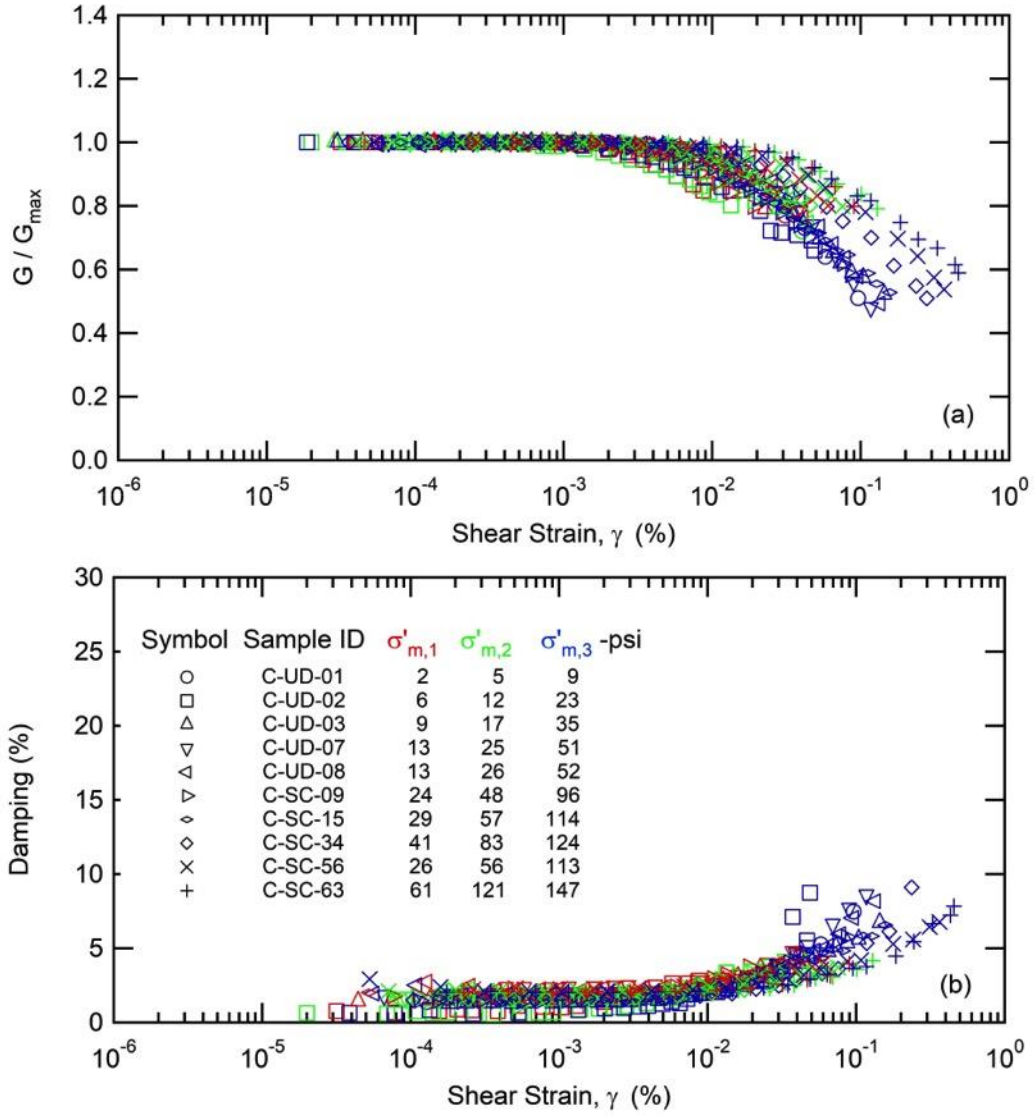

Figure 4.14 TS Testing Results for Soil Samples from Site A: (a) G/G_{max} Curves, and (b) Damping Curves

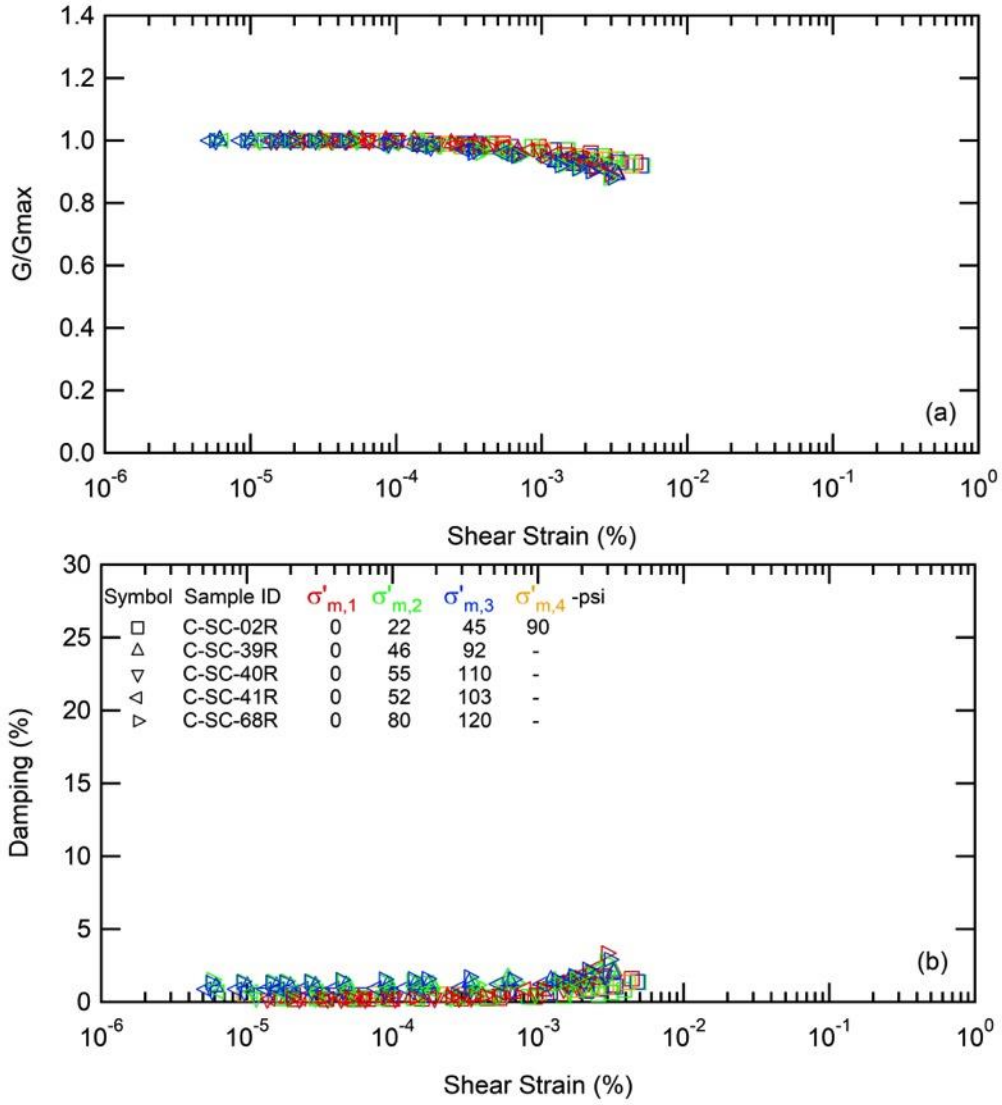

Figure 4.15 RC Testing Results for Rock Samples from Site A: (a) G/G_{max} Curves, and (b) Damping Curves

4.4.2. Dynamic Behaviors of Materials from Site B

RC and TS tests were performed on five samples from Shelby tubes and fifteen samples from the core sampler. The material properties and testing confinements are presented in Table 4.4. Soil samples were mostly sand for the depths of 5-10 ft, and clay or silt with high plasticity index at the depths below 150 ft. Sample A-UD-03 and A-UC-05 were tested at dry state prepared by reconstitution as discussed in Section 3.3.3. Rock samples were classified as either sandstone or claystone.

Table 4.4 Material Properties of Tested Samples for Site B

Sample ID[1]	Depth (ft)	σ'_{mo}[2] (psi)	Soil / Rock Type	%Finer	PI	ω_i[3] (%)	ω_f[4] (%)	Total Unit Weight (lb/ft^3)	σ'_m[5] (psi)
A-UD-01	5	2	SC	30.5	27	22.6	17.6	127	1, 2, 4
A-UD-02	7	3	SM	23.2	1	14.3	13.9	109	3, 5, 11
A-UD-03*	9	3	SM	14.3	np[6]	0.0	0.0	110	3, 7, 13
A-UD-05*	150	41	SP	0.0	np	0.0	0.0	92	21, 41, 83
A-UD-06	153	43	ML	57.5	11	26.0	23.5	121	22, 43, 86
A-SC-27	153	43	CL	64.2	13	33.3	30.2	120	22, 43, 86
A-SC-49	253	68	CH	68.0	33	30.2	24.8	119	34, 68, 136
A-SC-77	393	110	MH	62.0	24	35.4	33.5	105	55, 110, 138
A-SC-86	438	122	CH	72.6	29	25.7	24.3	121	31, 61, 122
A-SC-96	488	136	CH	74.9	33	31.3	30.9	119	32, 68, 136
A-SC-105	533	148	SC	42.9	20	25.6	22.1	121	37, 74, 111
A-SC-42R	218	68	Sandstone	-	-	-	-	161	0, 34, 68, 135
A-SC-52R	268	89	Sandstone	-	-	-	-	160	0, 45, 89, 133
A-SC-59R	303	100	Claystone	-	-	-	-	152	0, 50, 100
A-SC-60R	308	98	Claystone	-	-	-	-	148	0, 49, 98
A-SC-109R	553	184	Sandstone	-	-	-	-	167	0, 46, 92
A-SC-110R	558	174	Sandstone	-	-	-	-	168	0, 44, 87, 130
A-SC-112R	568	177	Sandstone	-	-	-	-	167	0, 44, 89
A-SC-115R	583	197	Sandstone	-	-	-	-	163	0, 49, 98
A-SC-116R	588	190	Sandstone	-	-	-	-	167	0, 47, 95

1. UD represents Shelby tube sample, and SC represents core sample; R is for rock sample

2. σ'_{mo} represents in-situ mean confining stress (K_0=0.5 assumed)

3. ω_i represents initial water content

4. ω_f represents final water content

5. σ'_m represents testing mean confining stress

6. np represents non-plastic

** reconstituted sample*

Results from RC and TS testing in terms of normalized modulus and damping for soil samples are presented in Figs. 4.16 and 4.17. Both tests were carried out between strain levels of 10^{-5}% to 0.5% and when G/G_{max} values reached approximately 0.5. The degradation of G/G_{max} curves for most of the samples occurred at strains 10^{-3} to 10^{-2}%. Damping values started to increase at strains higher than 10^{-2}%. Samples A-UD-01, A-UD-02, and A-UD-03 behaved more nonlinearly than other samples. This may be a result of testing these samples at very low confinement. Therefore, results for both G/G_{max} and damping at high strains at depths of 5-10 ft could vary greatly due to non-linear behavior and should be used along with other data to make design parameter selection.

Results for RC testing for rock samples are presented in Fig. 4.18 Similar to rock testing results from Site A, a very slight effect of confinement was observed. Relatively higher damping was observed for three samples A-SC-59R, A-SC-60R, and A-SC-115R. It was noted that samples A-SC-59R and A-SC-60R were classified as claystone, whereas sample A-SC-115R (i.e., sandstone)

appeared to contain some amount of fines within the sandstone matrix. Photos of these samples are shown in Fig. 4.19.

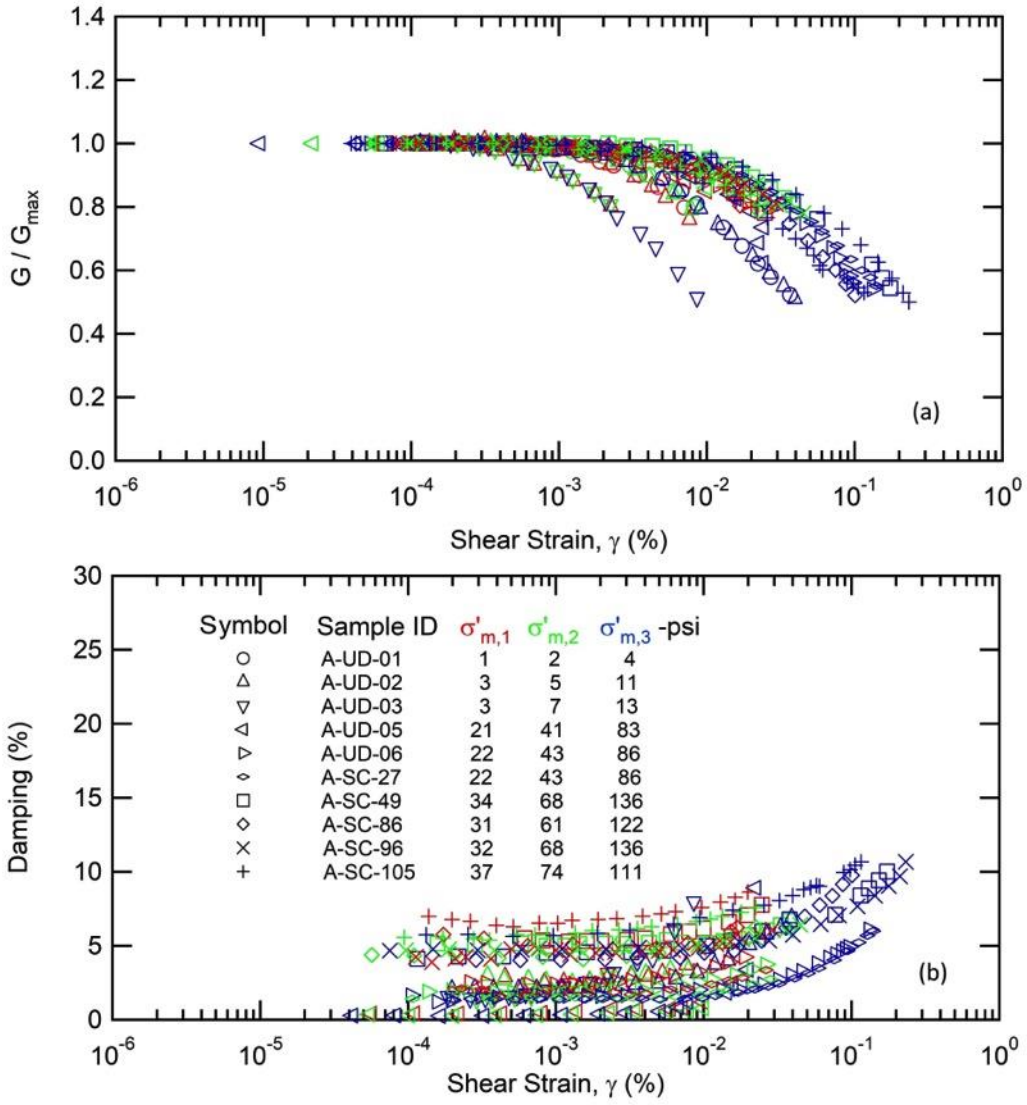

Figure 4.16 RC Testing Results for Soil Samples from Site B: (a) G/G_{max} Curves, and (b) Damping Curves

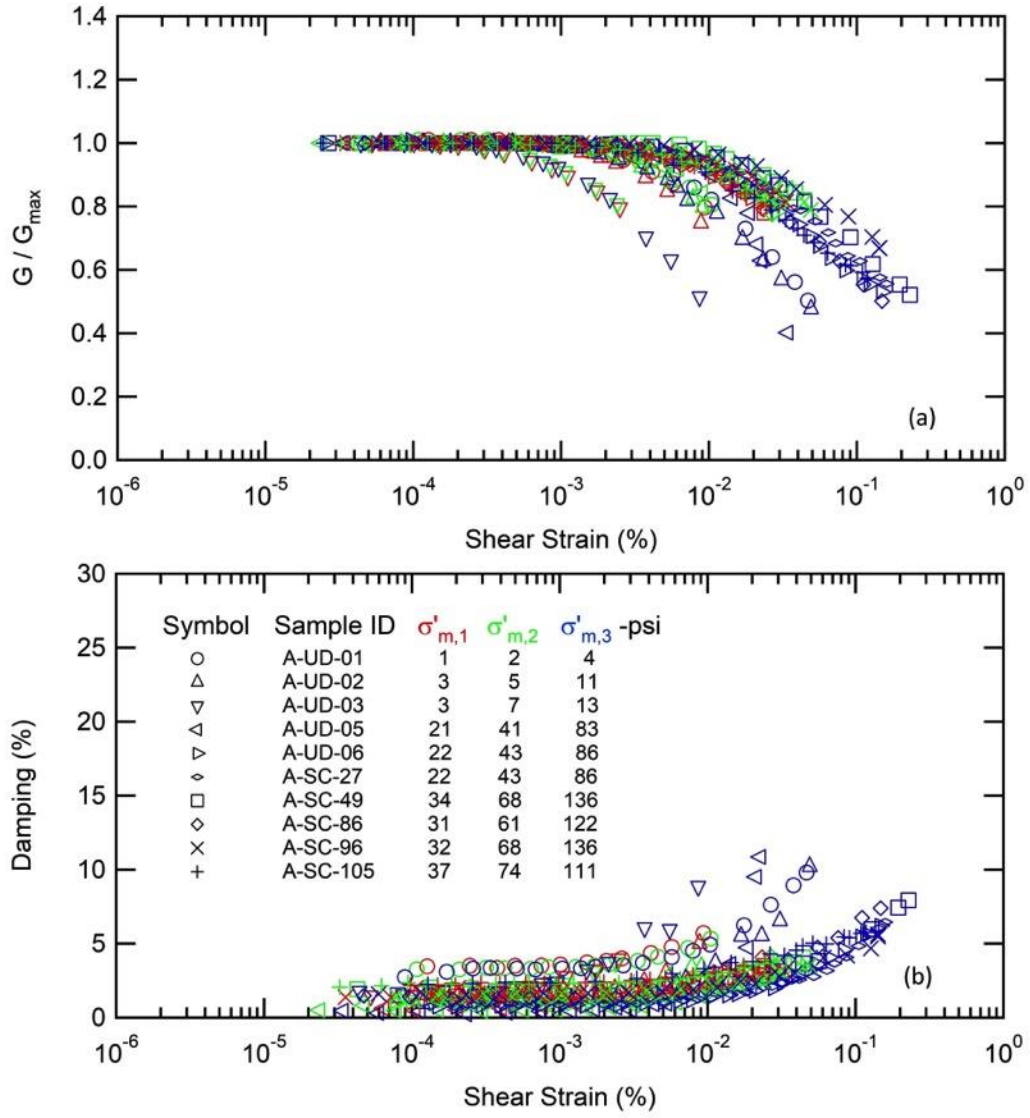

Figure 4.17 TS Testing Results for Soil Samples from Site B: (a) G/G_{max} Curves, and (b) Damping Curves

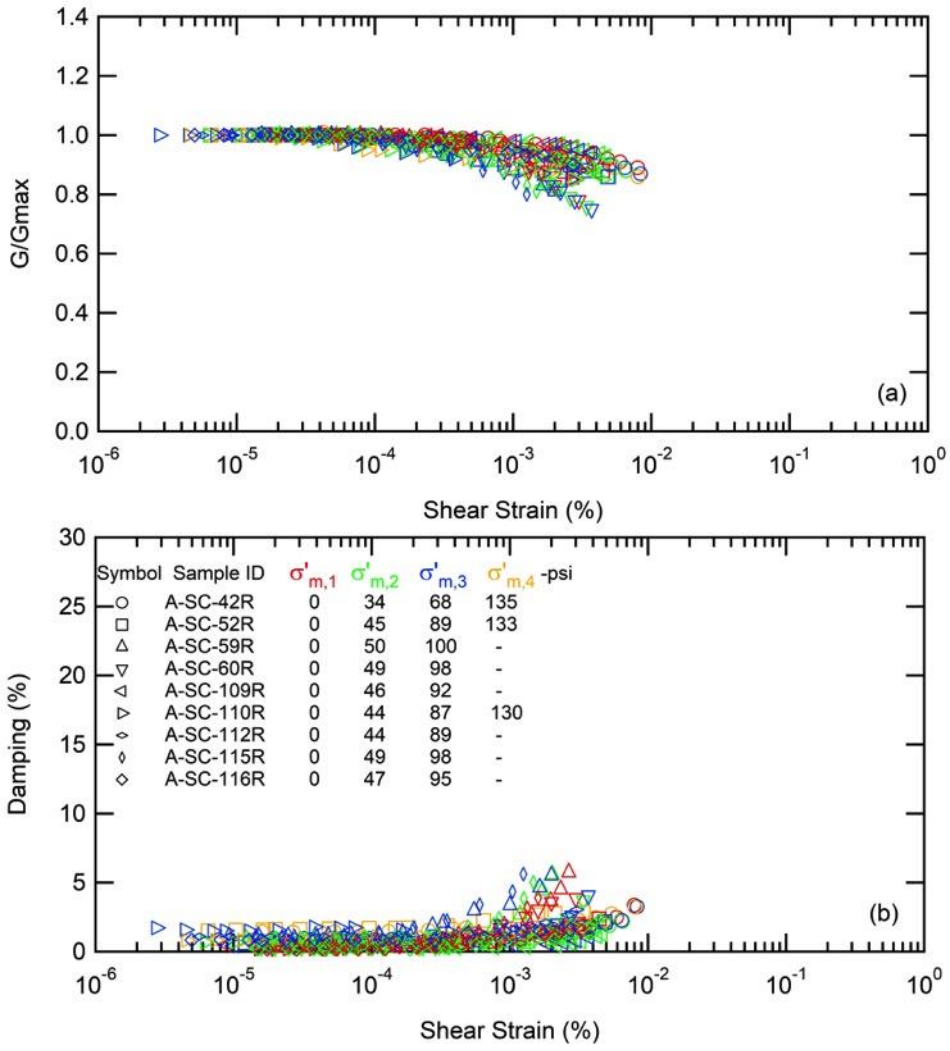

Figure 4.18 RC Testing Results for Rock Samples from Site B: (a) G/G_{max} Curves, and (b) Damping Curves

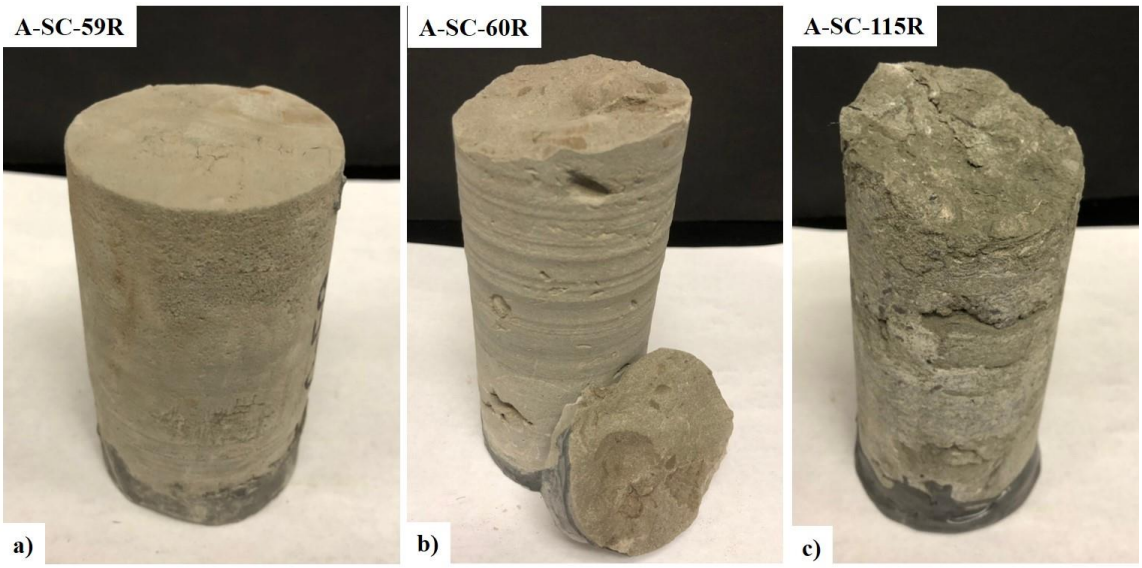

Figure 4.19 Photos of Rock Samples that Exhibited Relatively High Damping

4.4.3. Data Analysis and Interpretation of Dynamic Soil Properties

This section presents further analysis of factors affecting the dynamic soil properties from both sites. These factors including confinement, testing frequency, geologic age, and soil plasticity are typical factors that have been studied extensively in the literature. Effects of these factors on the dynamic properties of soils from the South Carolina Coastal Plain deposits are discussed.

4.4.3.1. Effect of Confinement

Shear wave velocities of soil and rock samples are presented in Figs. 4.20 and 4.21 for Sites A and B, respectively. At both sites, the V_s ranged from 540 to 1280 ft/s for the soil samples and from 4100 to 4300 ft/s for the rock samples for the confinement ranging from zero to a maximum of 140 psi. Effects of confinement on V_s were observed to be minimal for the rock samples as the V_s increased with confinement by approximately less than 1% from zero to 140 psi confinement. For the soil samples, V_s increased by 2-5 ft/s per increment of 1 psi confinement. It should be noted that this observation does not account for soil properties, geological age, and other factors.

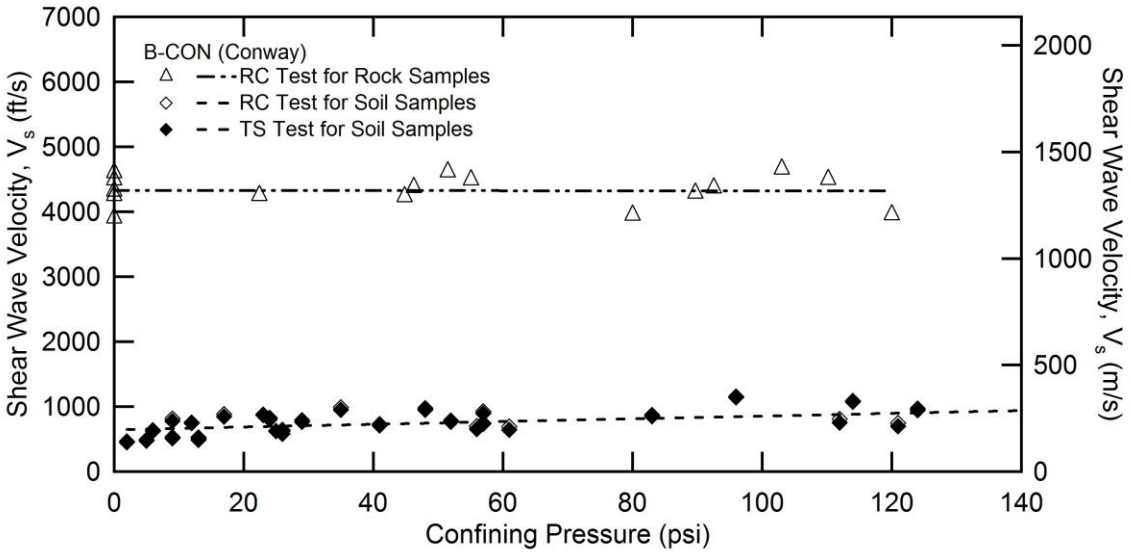

Figure 4.20 Variation of Shear Wave Velocity with Confinement for Site A

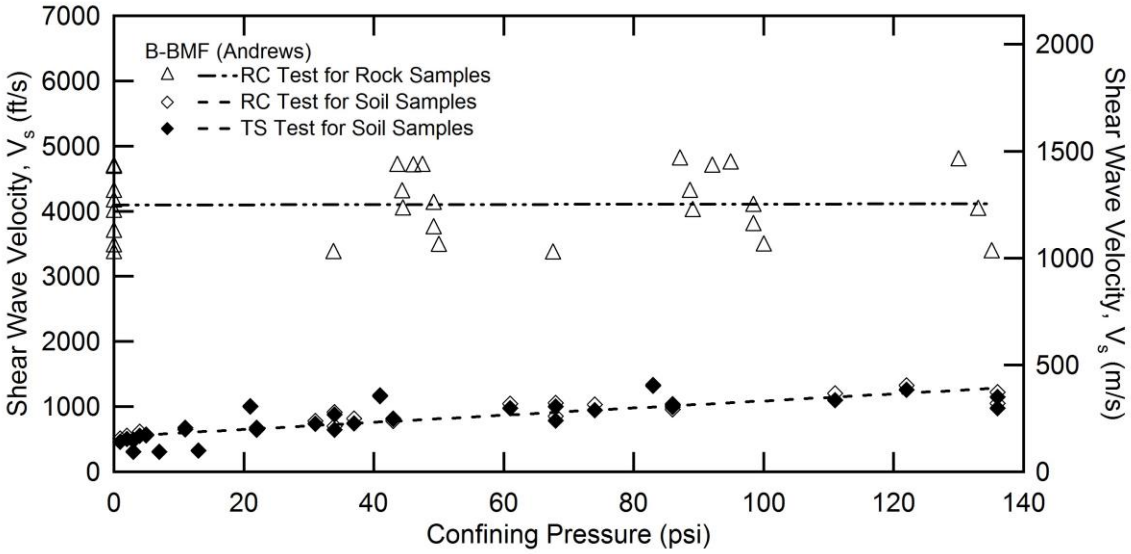

Figure 4.21 Variation of Shear Wave Velocity with Confinement for Site B

As shown in Figs. 4.22 and 4.23, the low-strain damping (D_{min}) ranged from 1.5 to 5% for the soil samples and from 0.2 to 1.2 % for the rock samples at both sites regardless of the testing method used. However, the data was more scattered compared with the V_s data in Figs 4.20 and 4.21. Furthermore, the data for the soil samples is less scattered in the TS testing results when compared to the RC testing results, and the effects of confinement were observed to be minimal. A large variation of damping for soil was due to the difference in testing frequency between RC and TS tests, which is discussed in Section 4.4.3.2.

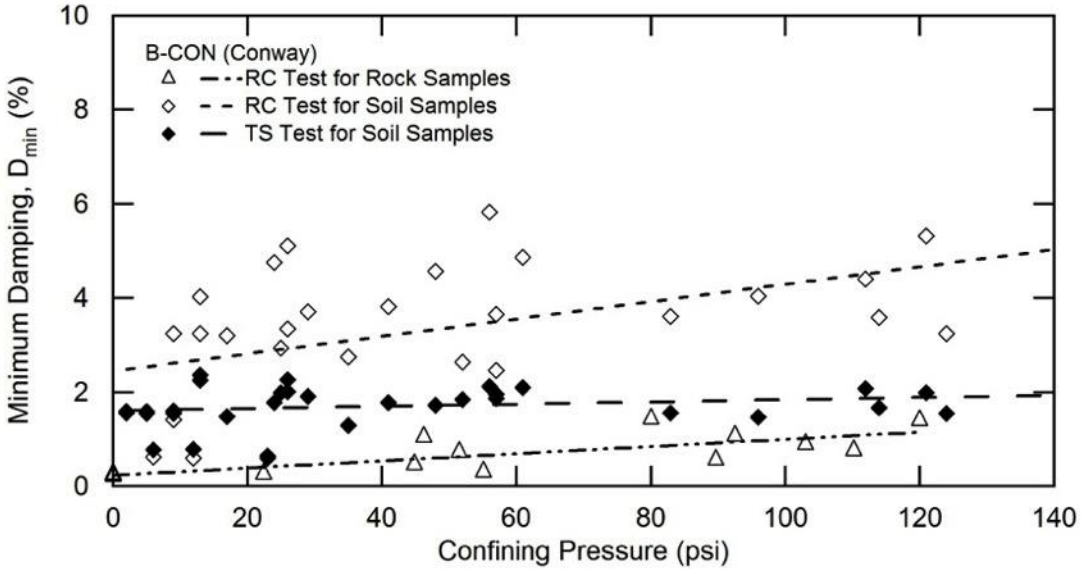

Figure 4.22 Variation of Damping with Confinement for Site A

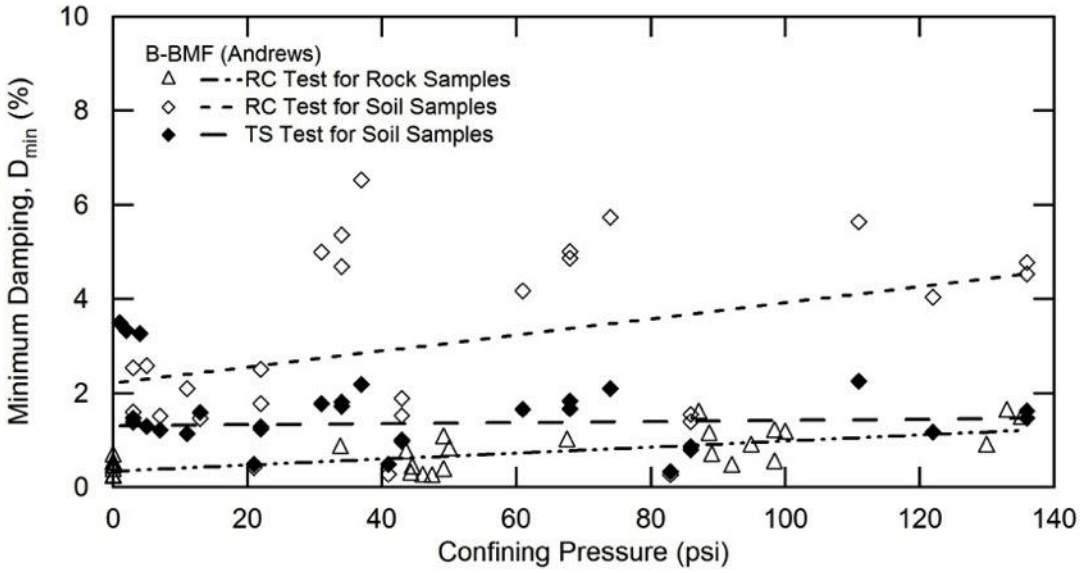

Figure 4.23 Variation of Damping with Confinement for Site B

The V_s results obtained from the RC tests at in-situ mean confining stress is presented in Tables 4.5 and 4.6 in comparison with the V_s data obtained from the three field methods. The results are separated into two groups: soil samples and cemented soil/rock samples. The V_s of the soil samples from the RC tests are lower than the results from the field tests. In contrast, the V_s of the cemented soil/rock samples are higher than the results from the field tests. Other contributing factors include the differences in stress conditions between the laboratory and the field, and sample disturbance. It is also important to note that the soil samples represent a wide variety of soil types including silty clay, clayey sand, and high plasticity clay or silt. These samples had relatively weak cementation. The cemented soil/rock samples were very hard and had some imperfections. In some samples, interbedded lenses of clay or silt were present, whereas some samples appeared to be solid hard rock. The higher V_s observed for the rock samples compared to those found with the field methods is possibly due to the fact that the solid rock sample was selected and tested without taking in to account the existence of rock fractures and interlayering system that exists in the field. Furthermore, laboratory testing provides dynamic soil properties and behaviors at higher strains (see Section 4.4.3.2) than field-testing which is limited to low strain.

Table 4.5 Comparison of V_s of Soil Samples for Site A

Sample ID	Depth (ft)	Soil/Rock Type	σ'_{mo} (psi)	Shear Wave Velocity (ft/s)			
				Resonant Column Test	MASW-MAM	MASW-SASW	P-S Suspension Logging
C-UD-01	11	CH	5	509	413	479	873
C-UD-02	16	SC-SM	6	635	413	466	873
C-UD-03	56	CH	17	989	846	1004	1719
C-UD-07	84	CH	25	736	1516	1204	1231
C-UD-08	87	CH	26	764	1516	1204	1231
C-SC-04R	133	Sandstone	45	4253	1557	1329	2383
C-SC-09	158	SC	48	1157	1557	1509	1537
C-SC-15	188	MH	57	1088	1557	1509	1444
C-SC-34	283	SC	83	873	1557	-	1480
C-SC-39R	308	Sandstone	93	4374	1557	-	1480
C-SC-40R	313	Sandstone	110	4490	1557	-	1934
C-SC-41R	318	Sandstone	103	4650	1557	-	1934
C-SC-56	393	CH	113	698	1659	-	1596
C-SC-63	428	CH	160	749	1659	-	1411
C-SC-68R	454	Sandstone	1101	3975	1659	-	2013

Table 4.6 Comparison of V_s of Soil Samples for Site B

Sample ID	Depth (ft)	Soil/Rock Type	σ'_{mo} (psi)	Shear Wave Velocity (ft/s)			
				Resonant Column Test	MASW-MAM	MASW-SASW	P-S Suspension Logging
A-UD-01	5	SC	2	614	708	699	-
A-UD-02	7	SM	3	477	708	699	-
A-UD-03	9	SM	3	304	708	699	-
A-UD-05	150	SP	41	1171	1582	1476	1441
A-UD-06	153	ML	43	1013	1582	1476	1441
A-SC-27	153	CL	43	956	1582	1476	1441
A-SC-42R	218	Sandstone	68	3349	1685	1476	1701
A-SC-49	253	CH	68	850	1685	-	1838
A-SC-52R	268	Sandstone	89	4000	1685	-	1838
A-SC-59R	303	Claystone	100	3465	1685	-	2115
A-SC-60R	308	Claystone	98	4072	1685	-	2115
A-SC-77	393	MH	110	797	1859	-	1849
A-SC-86	438	CH	122	1321	1859	-	1849
A-SC-96	488	CH	136	1218	1859	-	1590
A-SC-105	533	SC	148	1367	1859	-	1930
A-SC-109R	553	Sandstone	184	4682	1859	-	1930
A-SC-110R	558	Sandstone	174	4827	1859	-	1930
A-SC-112R	568	Sandstone	177	4290	1859	-	1930
A-SC-115R	583	Sandstone	197	3875	2361	-	2057
A-SC-116R	588	Sandstone	190	4777	2361	-	2057

4.4.3.2. Effect of Testing Frequency

The frequency effects on low-strain shear modulus and damping of selected soil samples from both sites were examined by conducting a series of TS tests at frequencies ranging from 0.001 and 2 Hz. To compare the effect of frequency, results were normalized with the results measured at a frequency of 0.5 Hz. In addition, the TS results are compared with the results from RC tests performed on the same soil sample at frequencies ranging from 20 to 50 Hz as shown in Fig. 4.24. For the shear modulus, the effect of frequency was found to be small (approximately 10%). In contrast, for the damping, the effect of frequency was found to be as high as 50-200%. It is therefore possible that results from RC tests can provide damping twice as much as the results from TS tests. Earthquake motion is composed of a wide range of frequencies. It is important that damping measurements should be performed using both RC and TS methods. Frequency effects on small strain dynamic properties have been recognized and studied by Stokoe et al. (1999), Rix and Meng (2005), and Ruttithivaphanich and Sasanakul (2019). However, the impact of frequency on site response analysis, especially the effect on damping, is not routinely accounted for in practice, and more research on this topic is needed. Because this study showed a pronounced effect of frequency on plastic fine grained soils (i.e. silty and clayey soils), and until further studies are conducted to develop predictive equations for the frequency effects on damping that can be used in practice, it is recommended to perform both RC and TS tests on soil samples to examine the effects of testing frequency on shear modulus and damping.

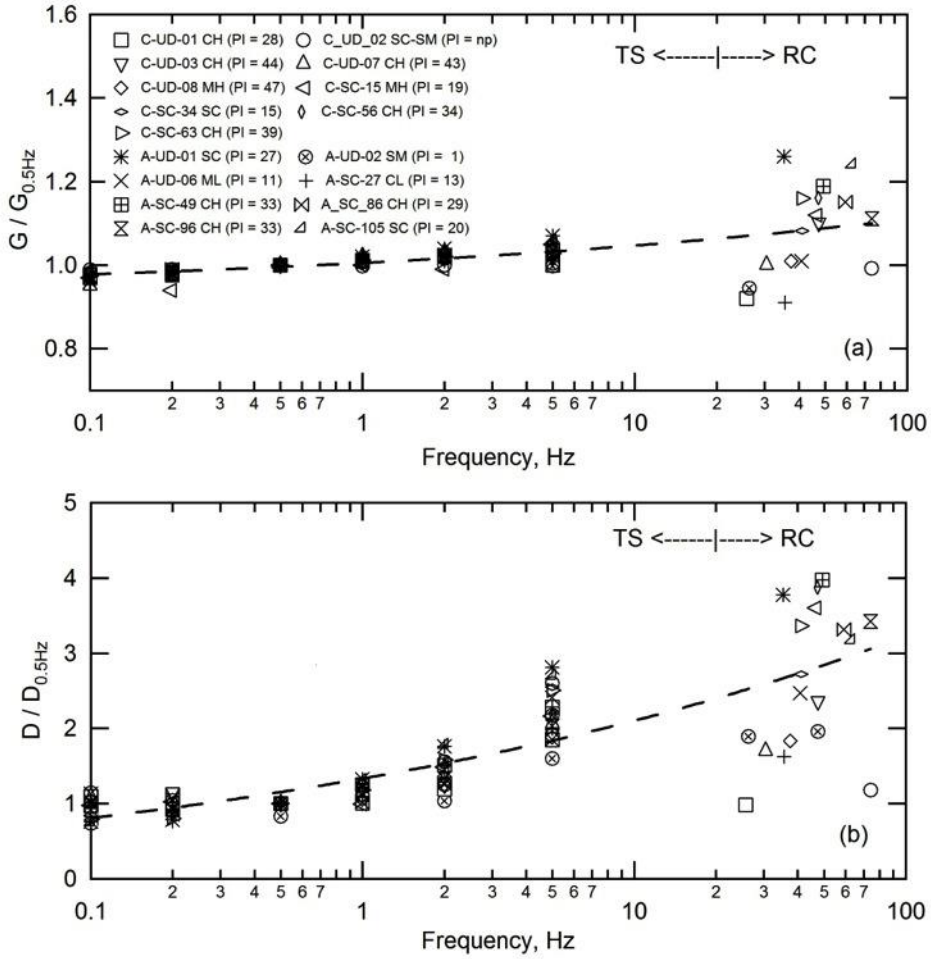

Figure 4.24 Effect of Testing Frequency on: (a) Normalized $G/G_{0.5Hz}$, and (b) Normalized $D/D_{0.5Hz}$

4.4.3.3. Effect of Geological Age and Soil Plasticity

Dynamic behaviors of soil and rock from both sites are separated into three geological age groups: Quaternary (Penholoway allo), Tertiary (Ashley or Cooper Marl), and Cretaceous (Peedee and Black Creek) deposits. Results from RC and TS tests are shown in Figs. 4.25, 4.26, and 4.27 for selected confinements. Results were compared with the empirical relationships proposed by Vucetic and Dobry (1991) for soils of varying plasticity as given by the plasticity index (PI). It is important to note that the Vucetic and Dobry (1991) relationships were obtained from soil tested at confining pressure of 0.25 to 4 atm (4 to 60 psi); therefore, the results should be compared at the confinement within +/- 50% range of the general curves as suggested by Stokoe et al. (1995). In addition, the proposed prediction procedure of G/G_{max} and damping curves for specific PI and confinement by Andrus et al. (2003) are plotted for comparison.

For the Quaternary age deposits, five soil samples were available as shown in Fig. 4.25. Comparing results for G/G_{max} curves with the Vucetic and Dobry (1991) curves with varying ranges of PI, the results aligned with curves for a range of PI that was higher than the PI of the soil samples tested. The rate of increasing in damping at high strains was higher than the Vucetic and Dobry (1991) curves. Comparing results for both G/G_{max} and damping curves with the Andrus et al. (2003) curves, the results agreed fairly well for the same range of PI and all strain levels. It is important to note that these samples had very little to no cementation.

For the Tertiary age deposits, results from a total of three soil samples and one rock sample are presented in Fig. 4.26. The overall results show the same trend in the slopes and on-set of nonlinearity as Vucetic and Dobry (1991); however, similar to the Quaternary age group, the G/G_{max} curves generally align with curves for a range of PI that was higher than, but not related to, the PI of these samples. For Sample A-UD-5, the rate of increasing in damping was higher than the Vucetic and Dobry (1991) prediction, but the results agree with the Andrus et al. (2003) curves.

The dynamic behavior of the low plasticity samples (A-SC-27 and A-UD-6) does not match the predicted behavior proposed by Andrus et al. (2003), but is similar to the high plasticity (PI equals 50) predicted behavior of Vucetic and Dobry (1991). It is interesting to observe that the nonlinear behavior of rock sample A-SC-42R was similar to the soil samples. Behaviors of soil and rock deviated from the empirical curves suggesting that the materials within the same age group can be highly variable.

Overall, there was no clear relationship between soil plasticity and both G/G_{max} and D for the soil samples tested herein. It is important to recognize that the soil preparation process for the measurement of the plastic and liquid limit to determine PI breaks down the structure of cemented soil. Therefore, the effects of PI on dynamic soil behavior may not be relevant to, or less dominant than, the effect of cementation. These findings are based on limited number of samples and therefore more data are needed to quantitatively evaluate the effects (e.g. amount and/or characteristics) of cementation on dynamic soil properties of older soil deposits typically found in the South Carolina Coastal Plain. Consequently, more accurate prediction of dynamic properties can be achieved.

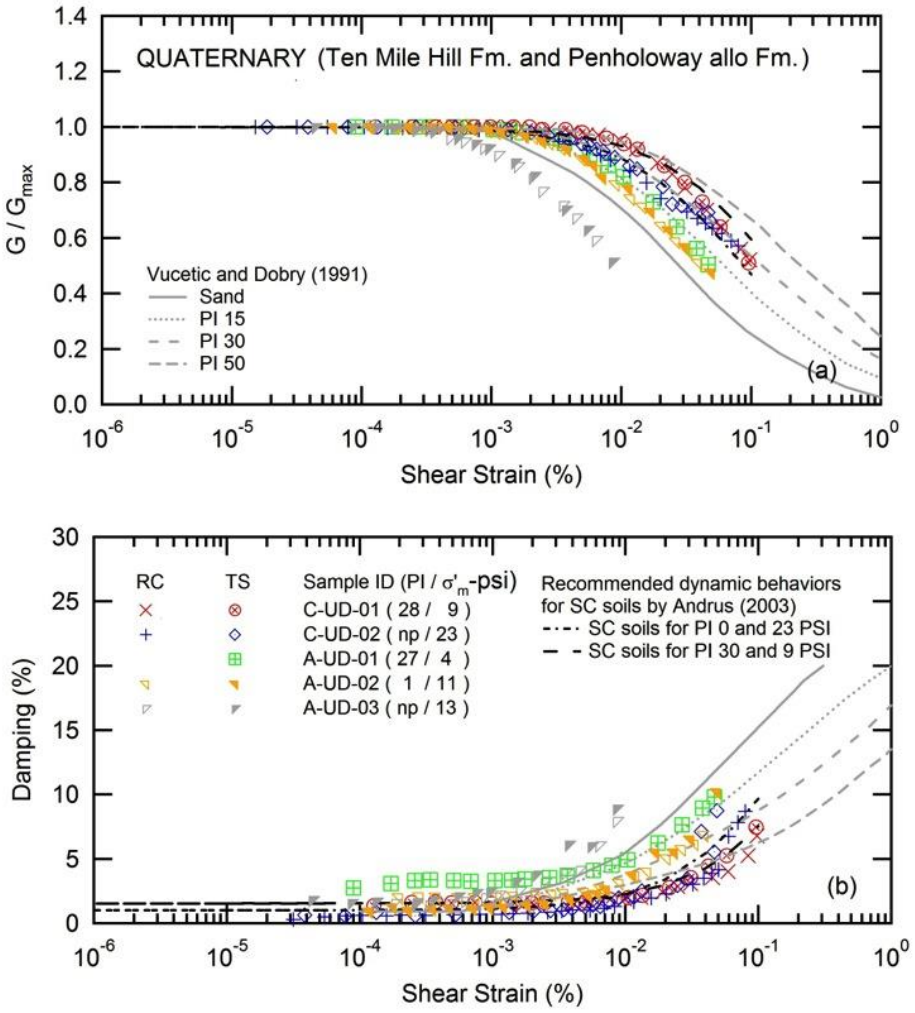

Figure 4.25 Dynamic Properties of Quaternary Age Soils: (a) G/G_{max} Curves, and (b) Damping Curves

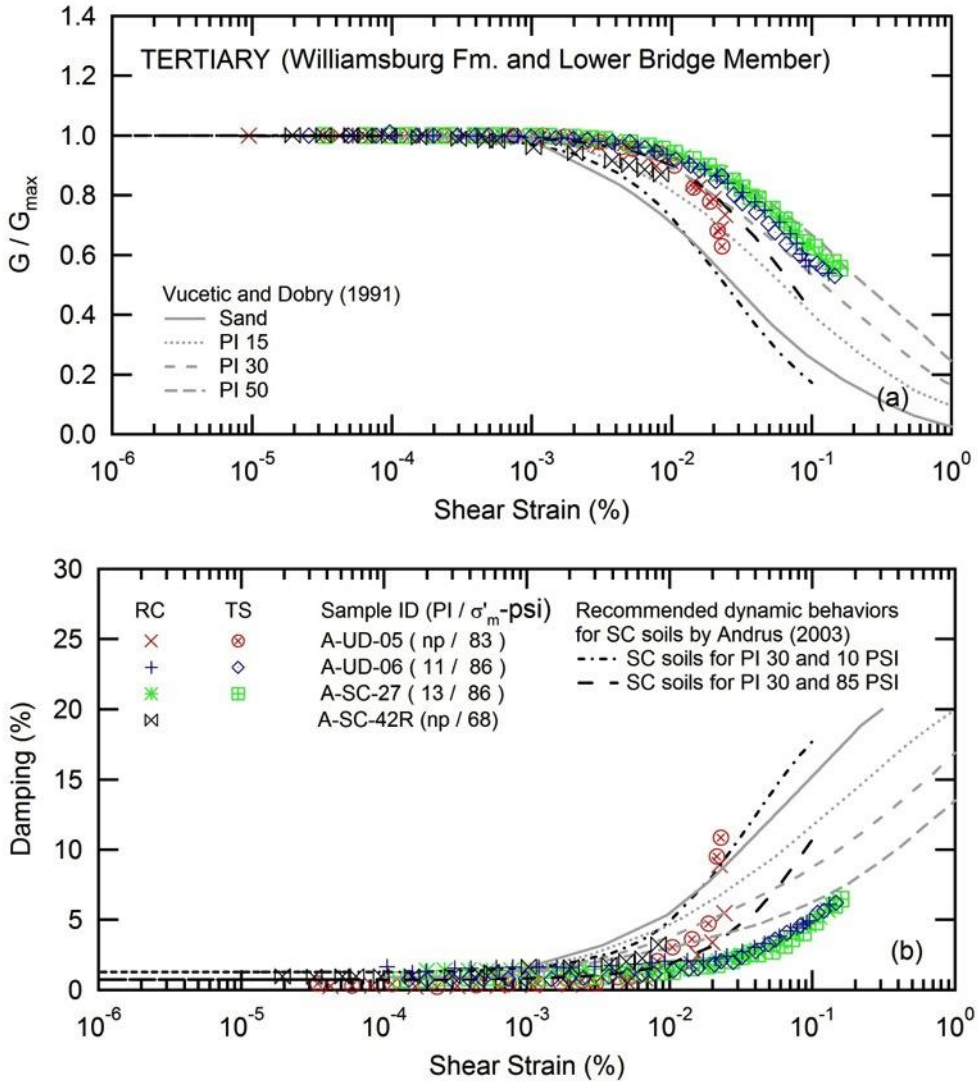

Figure 4.26 Dynamic Properties of Tertiary Age Soils: (a) G/G_{max} Curves, and (b) Damping Curves

For the Cretaceous age deposits, the results are compiled from a total of 12 soil samples and 13 rock samples as presented in Fig. 4.27. It is interesting to observe that the G/G_{max} curves from some of the rock samples started to degrade at lower strains than the soil samples. Overall, the results are plotted within the predicted curves by Vucetic and Dobry (1991) for PI between 30 to 100; hence, the results aligned with curves for a range of PI that was higher than the PI of these samples. Again, there was no clear trend for the effect of plasticity on both G/G_{max} and D for the soil samples tested herein. Rock samples appeared to behave more nonlinearly than soil samples. In general, results for D_{min} were higher than the prediction by Vucetic and Dobry (1991) and similar to the results for Quaternary and Tertiary age groups; the rate of increasing in damping was

higher at higher-strain levels. There was no prediction for Cretaceous age soil according to Andrus et al. (2003), therefore this set of data can be used to improve and expand the SCDOT database for older age soils.

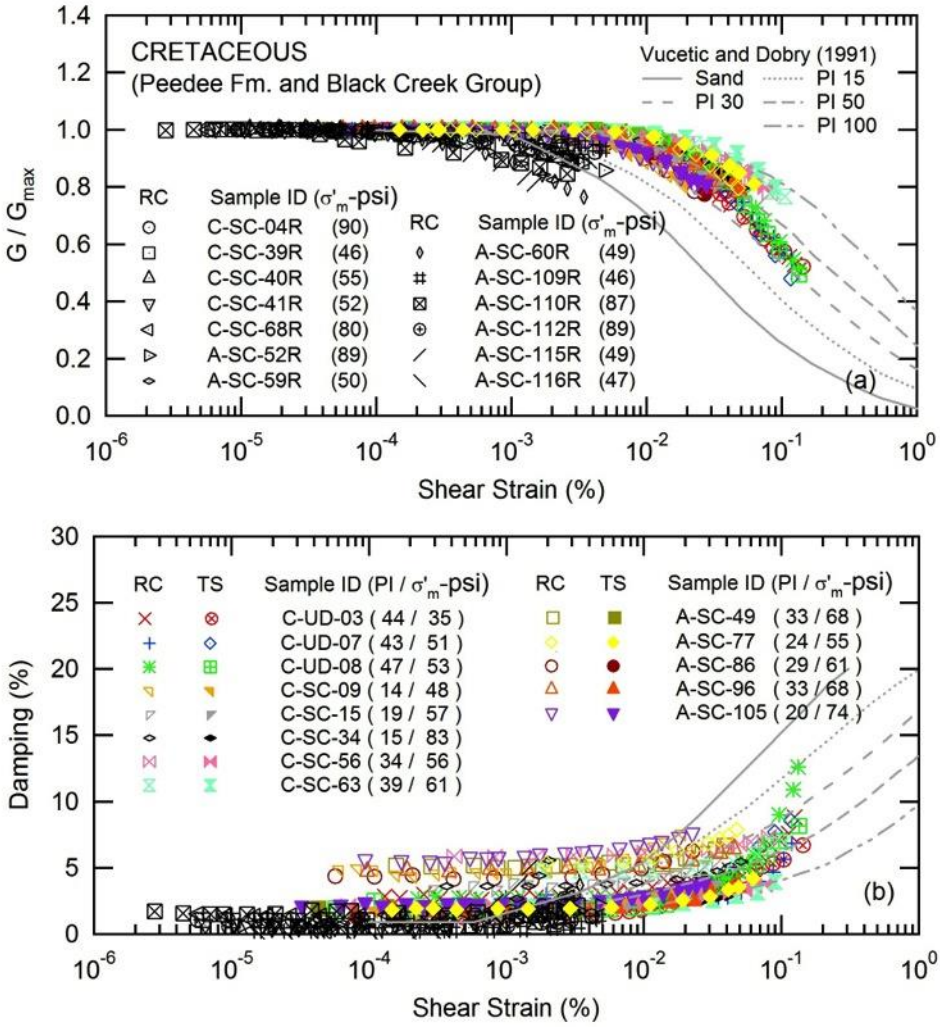

Figure 4.27 Dynamic Properties of Cretaceous Age Soils: (a) G/G_{max} Curves, and (b) Damping Curves

4.4.3.4. Statistical Analysis of Predictive G/G_{max} and Damping Curves

As mentioned in the previous section, the predictive G/G_{max} and damping curves proposed by Andrus et al. (2003) matched only some of the results for the samples of Quaternary and Tertiary age that were tested in this study. Furthermore, Andrus et al. (2003) did not develop predictive curves for the Cretaceous age, of which the majority of the samples tested in this study were from. Since the samples in this study were taken from different locations and geologic formations than those used by Andrus et al. (2003), new predictive curves were developed and assessed for the

new set of data obtained in this study. The same approach of Andrus et al. (2003) was utilized for this effort.

In accordance to the Andrus et al. (2003) procedure, only TS results for soils are used to minimize frequency effects on damping. It is noted that the G/G_{max} curves for RC and TS tests for soils are relatively close but the low-strain damping for TS tests are lower. For rock samples, RC test results are used because TS test results are not available. The procedure is described below.

The modified hyperbolic model (Stokoe et al. 1999 and Darendeli 2001) was proposed for the G/G_{max} curves as:

$$\frac{G}{G_{max}} = \frac{1}{1+\left(\frac{\gamma}{\gamma_r}\right)^{\alpha}} \tag{4.1}$$

where G is the shear modulus, G_{max} is the low-strain shear modulus, γ is the shear strain, γ_r is the reference strain, and α is the curvature coefficient. Curve fitting function parameters (γ_r and α) were obtained from the G/G_{max} curves. The reference strain was corrected for the effect of confinement using the following equation.

$$\gamma_r = \gamma_{r1}(\sigma'_m/P_a)^{k_\gamma} \tag{4.2}$$

where σ'_m is the mean effective confining stress in units of psi, P_a is a reference pressure of 14.5 psi, and k_γ is an exponent that varies with geologic formation and PI for shear modulus. It is noted that Andrus et al. (2003) uses k instead of k_γ.

To model the damping curves in relation to G/G_{max}, the quadratic polynomial function accounting for the corresponding G/G_{max} function proposed by Andrus et al (2003) was adopted and presented as:

$$D - D_{min} = A\left(G/G_{max}\right)^2 + B\left(G/G_{max}\right) + C \tag{4.3}$$

where D is the damping, D_{min} is the low-strain damping, and A, B, and C are curve fitting parameters. Andrus et al. (2003) proposed A= 12.2, B= -34.2 and C = 22 for R^2 = 0.785-0.960 based on data from the Savannah River Site and Charleston (see Figure 2.2).

In this study, soil and rock samples from Sites A and B were from the Quaternary (Ten Mile Hill and Penholoway alloformation), Tertiary (upper soil and Williamsburg Formation and Lower Bridge Member) and Cretaceous (Peedee Formation and Black Creek Group) age groups. Curve fitting was performed resulting in the parameters: A = 14.92, B = -35.99, and C = 21.34 for R^2 = 0.789 for soil, and parameters: A = 25.65, B = -61.92, and C = 36.40 for R^2 = 0.611 for rock.

Furthermore, the D_{min} was corrected for the effect of confinement similar to γ_r, by using:

$$D_{min} = D_{min1}(\sigma'_m/P_a)^{-k_D/2} \quad (4.4)$$

where k_D is an exponent for damping that varies with geologic formation and PI according to Andrus et al. (2003). It is noted that Andrus et al. (2003) assumed $k = k_\gamma = k_D$. D_{min1} is the low-strain damping at σ'_m of 14.5 psi presented as:

$$D_{min1} = a(PI)+b \quad (4.5)$$

where a and b are fitting parameters.

Curve fitting was performed to obtain 5 different model parameters: α, γ_{r1}, k_γ, k_D, and D_{min1}. The model parameters and R^2 are presented in Tables 4.7-4.9 as a function of PI for each geologic unit. It is noted that the results from curve fitting using data for all soils in each geologic unit is also presented for a comparison. Statistical analyses of the curve fitting are presented in Appendix G. Overall, the R^2 values for k_γ vary from 0.24 - 0.83 and the R^2 values for k_D vary from 0.09 – 0.81 for soils. When data from the same age group are combined for all soils, the R^2 values become lower. In addition, the R^2 values for rocks are very low (0.006-0.383). No clear trend was observed for the curve fitting parameters indicating that the dynamic behaviors of these samples are not dependent on PI and/or geologic group. Based on the visual observation and geological logging information of these samples, cementation could be one major factor affecting the dynamic soil properties. As mentioned in Section 4.4.3.3, further quantification of cementation (e.g. by weight) and qualitative evaluation (e.g. types and bonding characteristics) could improve understanding of the sample behavior. However, such studies were outside the scope of this project and thus, findings remain inconclusive.

Table 4.7 Model Parameters for Quaternary Deposit (Ten Mile Hill and Penholoway Formation)

Geologic Unit	QUATERNARY (Ten Mile Hill Formation and Penholoway alloformation)							
Age	2.6 - 0.01 MYA							
PI	Non-Plastic	1 -10	11 - 20	21 - 30	31-40	41-50	All Soils	Rock
γ_{r1} (%)	0.035	-	-	0.130	-	-	0.041	-
k_γ	0.477	-	-	0.575	-	-	0.221	-
$R^{2,*}$	0.211	-	-	0.589	-	-	0.048	-
D_{min1} (%)	0.779	-	-	1.374	-	-	0.845	-
k_D	0.740	-	-	0.680	-	-	0.960	-
$R^{2,**}$	0.616	-	-	0.361	-	-	0.542	-
α	1.118	-	-	1.237	-	-	1.165	-
No. of Sample	3	-	-	2	-	-	5	-

$R^{2,*}$ is a result of curve fitting in Eq. 4.2, $R^{2,**}$ is a result of curve fitting in Eq. 4.4.

Table 4.8 Model Parameters for Tertiary Deposit (Williamsburg Formation and Lower Bridge Member)

Geologic Unit	TERTIARY (Williamsburg Formation and Lower Bridge Member)							
Age	58.0 - 56.0 MYA							
PI	Non-Plastic	1 -10	11 - 20	21 - 30	31-40	41-50	All Soils	Rock*
γ_{r1} (%)	0.015	-	0.058	-	-	-	0.035	-
k_γ	0.647	-	0.552	-	-	-	0.619	-
$R^{2,*}$	0.891	-	0.831	-	-	-	0.249	-
D_{min1} (%)	0.572	-	1.418	-	-	-	1.023	-
k_D	0.272	-	0.634	-	-	-	0.472	-
$R^{2,**}$	0.810	-	0.928	-	-	-	0.131	-
α	1.300	-	1.065	-	-	-	1.143	-
No. of Sample	1	-	2	-	-	-	3	-

$R^{2,*}$ is a result of curve fitting for Eq. 4.2, $R^{2,**}$ is a result of curve fitting for Eq. 4.4, *the rock data is not included as there is only one sample in this age group.

Table 4.9 Model Parameters for Cretaceous Deposit (Peedee Formation and Black Creek Group)

Geologic Unit	CRETACEOUS (Peedee Formation and Black Creek Group)							
Age (MYA)	83.6 - 66.0 MYA							
PI	Non-Plastic	1 -10	11 - 20	21 - 30	31-40	41-50	All Soils	Rock***
γ_{r1} (%)	-	-	0.080	0.049	0.062	0.086	0.078	0.038
k_γ	-	-	0.364	0.422	0.794	0.243	0.461	0.163
$R^{2,*}$	-	-	0.578	0.677	0.572	0.540	0.447	0.006
D_{min1} (%)	-	-	2.224	2.087	2.080	1.862	1.978	0.156
k_D	-	-	0.220	0.272	0.130	0.086	0.090	-1.833
$R^{2,**}$	-	-	0.312	0.113	0.089	0.014	0.416	0.383
α	-	-	1.042	1.252	1.150	1.290	1.183	0.782
No. of Sample	-	-	4	2	4	3	13	13

$R^{2,*}$ is a result of curve fitting for Eq. 4.2, $R^{2,**}$ is a result of curve fitting for Eq. 4.4, ***only RC test was performed on rock sample.

Figs. 4.28 to 4.30 show examples of the predicted G/G_{max} and damping curves for the confining pressure of 14.5 psi. Due to limited data for the Quaternary and Tertiary age groups, it is recommended that lower bound and upper bound curves be used for the site response analysis for these groups. For the Cretaceous group, the effects of PI are not clearly observed, but the G/G_{max} and D curves for all samples fall within a narrow range and it is suggested that the average curves be used for the site response analysis. For the rock samples, the G/G_{max} curve degraded at much lower strains than the soil samples. This indicates that the rock may be stiff but brittle. If thick layers of soft rock (or highly cemented soil) are present at a site, it is recommended that RC and TS tests be performed to verify the behavior at medium to high strains. The damping curve for rock samples is observed to be lower than soils. Furthermore, it is important to note that the soil and rock curves were developed for strains up to 10^{-1}% and 10^{-2}%, respectively; therefore, extrapolation beyond these strain levels should be performed with caution.

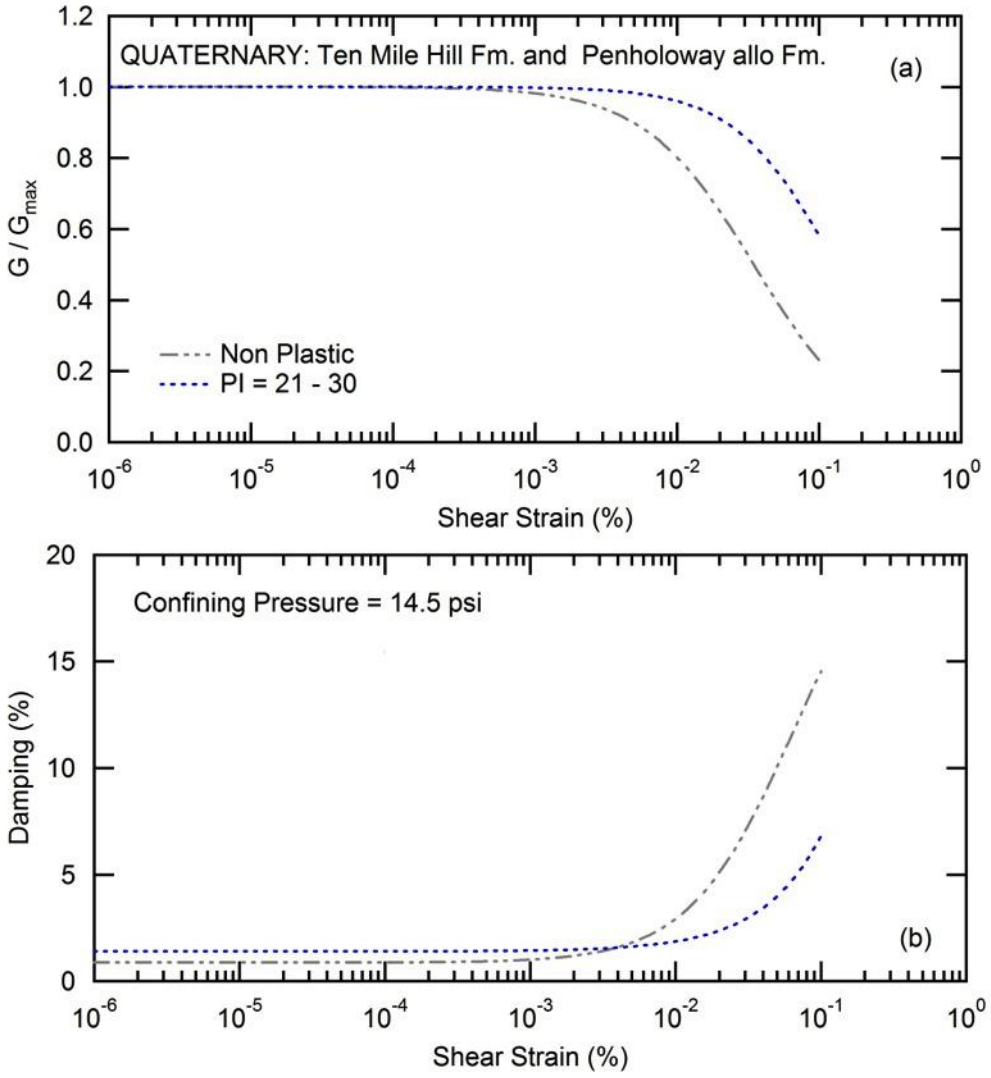

Figure 4.28 (a) G/G_{max} Curves, and (b) Damping Curves Generated from Predictive Model for Quaternary Age Soils: Ten Mile Hill Formation and Penholoway Alloformation

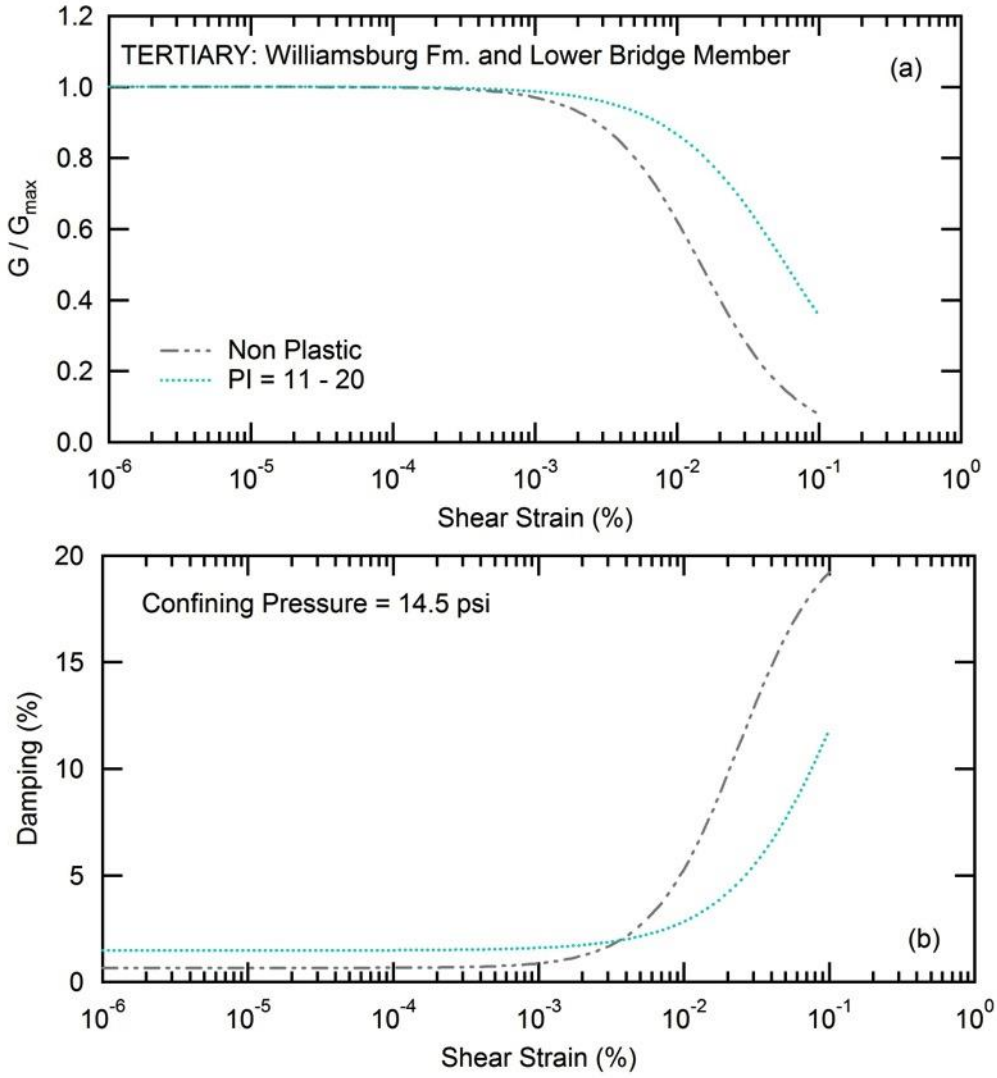

Figure 4.29 (a) G/G_{max} Curves, and (b) Damping Curves Generated from Predictive Model for Tertiary Age Soils: Williams Burg Formation and Lower Bridge Member

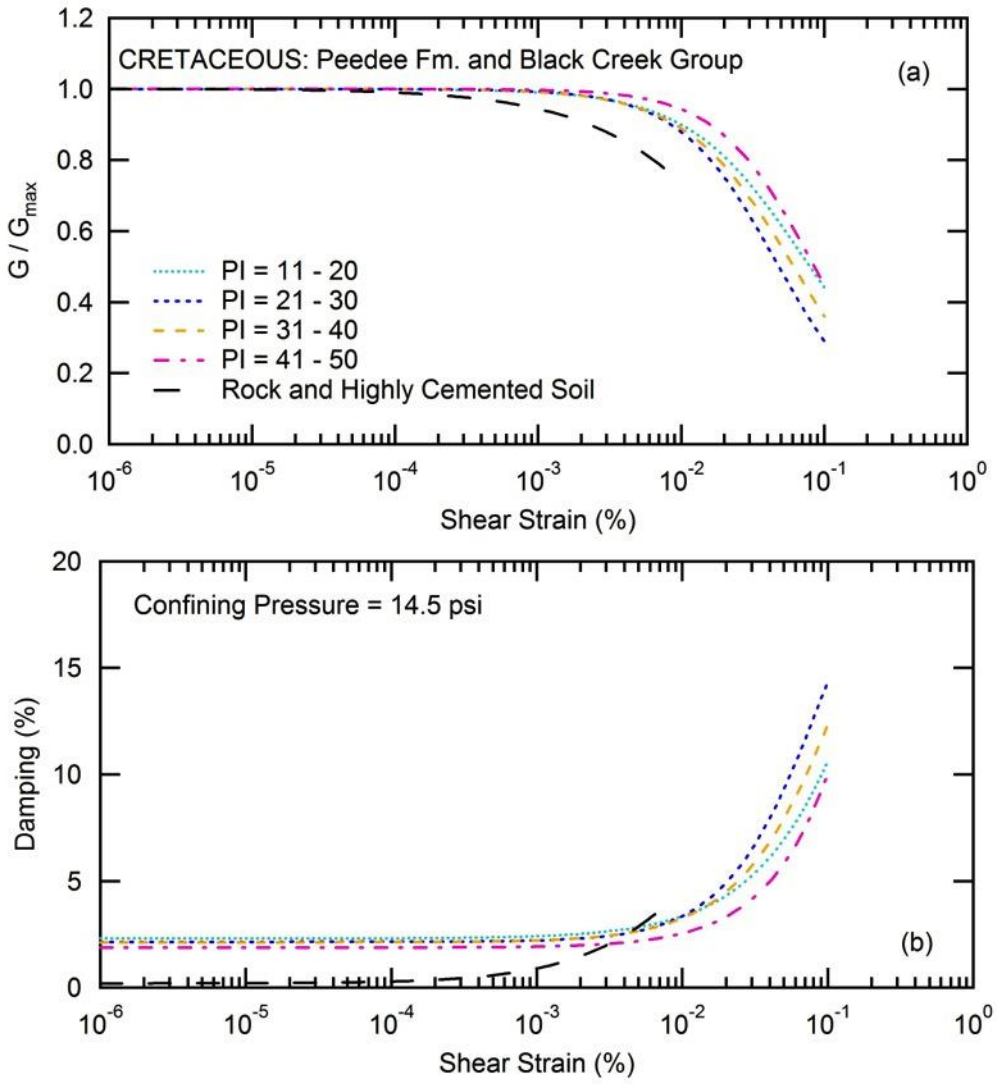

Figure 4.30 (a) G/G_{max} Curves, and (b) Damping Curves Generated from Predictive Model for Cretaceous Age Soils: Peedee Formation and Black Creek Group

The effect of soil plasticity on damping at low-strains (D_{min}) for the Quaternary, Tertiary and Cretaceous age soils are presented with the relations developed by Andrus et al. (2003) in Fig. 4.31. Results from this study (shown in solid symbols) were limited to PI values up to approximately 50; whereas, Andrus et al. (2003) had data up to 120. Low-strain damping for both geologic ages showed small increases as the PI increased. The rate of increase for the relationship for Tertiary age soils tested in this study was comparable with the trend proposed by Andrus et al. (2003). However, the new set of data generated for Cretaceous age deposits showed less variation with PI, and damping values were higher than Tertiary, Pleistocene, and Holocene age groups. It is important to understand that the majority of the data utilized by Andrus et al. (2003) came from tests performed on soil samples obtained from the Savannah River site. Although these samples

may be from the same or comparable geologic age, the characteristics and behavior of different deposits and formations can be vastly different. For example, sediments of the Peedee Formation may have been deposited in fluvial to delta-plain environments in the western part of the state; whereas, during the same time period, were deposited in shelf environments on the eastern side. The Peedee Formation at Sites A and B consists of a very fine- to coarse-grained, poorly sorted, massive calcareous clayey sands that are rich in shell and nanofossils fragments and with trace amounts of mica, whereas the Peedee Formation at the Savannah River site consists of light-colored fine- to coarse-grained quartz sand and oxidized kaolinite clay (Gellici 2019, Self-trail et al. 2002, Christopher and Prowell 2002, and Fallaw and Price 1995). This information supports the findings in this study that PI and geologic age alone are not dominant factors affecting the dynamic soil properties for older soil deposits, particularly for those samples with cementation. It is highly recommended that the SCDOT continue to collect more data and conduct further detailed geotechnical and geological investigations to characterize soils and rocks particularly for Tertiary and Cretaceous age deposits.

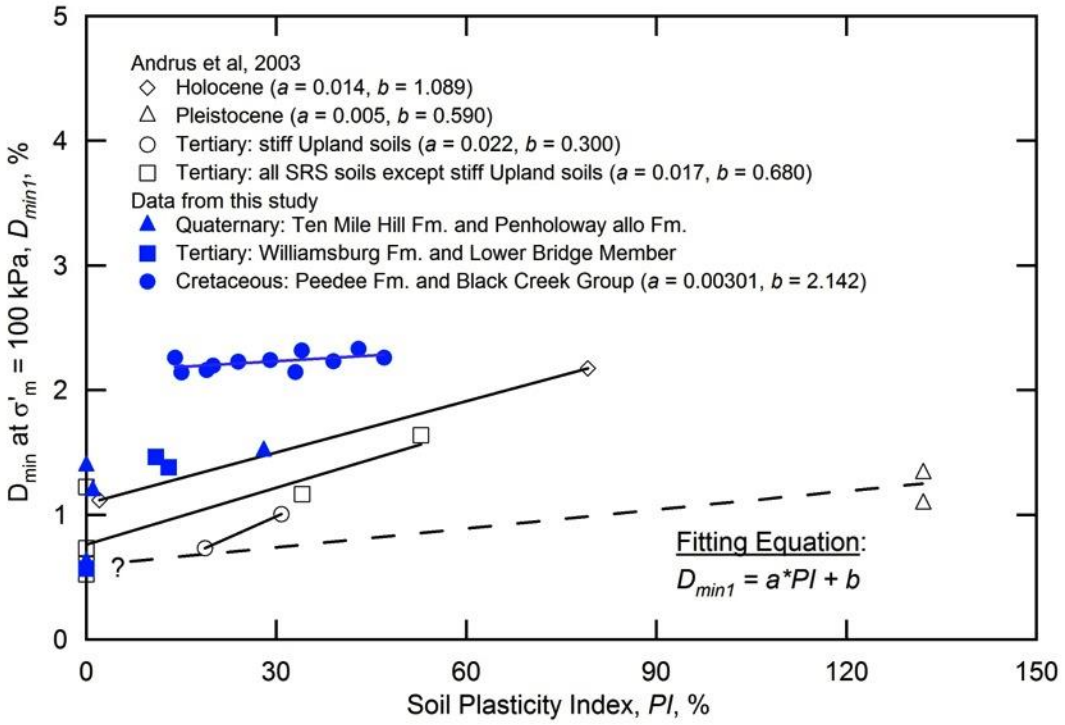

Figure 4.31 Variation of D_{min} with PI for Soils of Different Geological Ages (after Andrus et al. 2003)

5. Conclusion, Recommendations, Implementation, and Future Research Needed

5.1. Conclusions

This research presents a study to obtain comprehensive field and laboratory measurements of shear wave velocity and dynamic soil properties for two sites in the South Carolina Coastal Plain: Site A is located near Conway in Horry County and Site B is located in Andrews in Williamsburg County. Geotechnical borings were drilled to depths of 505 and 615 ft for Sites A and B, respectively. Shear wave velocity profiles were generated using P-S suspension logging, FWS logging, combined MASW-SASW, and combined MASW-MAM methods. The profiles using P-S suspension logging were obtained to a depth of 470 ft for Site A and a depth of 600 ft for Site B. Profiles to a depth of 220 ft were obtained from the MASW-SASW method for both sites. For the combined MASW-MAM method, profiles were obtained to a depth 4921 ft for Site A and a depth of 2625 ft for Site B. Overall, the average shear wave velocities obtained from the surface methods at the top 200 ft were lower than that of the P-S suspension logging data. This resulted in a different NEHRP site class when using the average V_s values in the top 100 ft for Site A, but not site B. The P-S suspension logging provided detailed characteristics of the soil profile within borehole(s) and the results agreed with the visual observation of samples. However, the P-S suspension logging method was not capable of measuring V_s at very shallow depths (approximately 6-11 ft in this study) and did not provide the depth of the B-C boundary as the boundary was below the bottom of each borehole. Both non-invasive surface methods were performed independently with different teams and these results were in agreement within the top 220 ft where the MASW-SASW results can be compared. The MASW-MAM method is a unique method utilizing passive ambient wave sources and specialized sensors that allows deep profiling and identified an estimated depth to the B-C boundary of 580 ft for Site A and 1343 ft for Site B. Results from both surface methods do show that spatial variation of both sites are high, especially for Site A. While the use of surface wave methods may be more attractive for site investigation as they are relatively lower cost compared to borehole methods, accurate results from the surface wave methods require geological and geotechnical knowledge of the site to effectively perform data processing. Since these methods are not direct measurements, the best representative V_s profile for each site relied on the experience and skill of the data analysts obtained from utilizing these methods at sites in South Carolina as well as other parts of the country. Furthermore, the V_s profiles from the surface wave methods represent the average profiles over a large volume of soil. Conversely, the V_s profiles from the borehole methods represent localized profiles within the tested borehole.

Visual observation of samples collected from both sites showed that materials were highly variable with frequent transitions between soil-like to rock-like material. In the Tertiary and Cretaceous deposits, materials with sand or clay structures with high variation of cementation and shell fragments were found. Highly cemented sand or clay (sandstone or claystone) with thickness

varying from a few inches to several feet was observed at several locations through the entire depth of the soil profiles investigated. The locations of these materials corresponded with the high shear wave velocities observed in the P-S logging profiles.

Resonant column and torsional shear testing allowed observation of shear modulus and damping behavior of material for a wide range of strains. A total of 35 soil and rock samples were tested and several factors affecting the small strain dynamic properties were investigated. Overall, it was found that the dynamic behavior aligned with the generic empirical prediction suggested by Vucetic and Dobry (1991) for a range of PI that was higher than the PI of these samples. Relatively high D_{min} values were observed and the rate of increasing in damping with strains was higher than the Vucetic and Dobry (1991) prediction. Damping was significantly affected by testing frequency therefore; results from the more common RC test obtained using high frequencies should be compared with results from TS tests at low frequencies. The effect of soil plasticity on the shear modulus reduction and damping curves for soils with different geological age groups was evaluated and found to have a smaller effect than predictions by previous studies for uncemented soils. The shear modulus of rock and highly cemented soils degraded at lower strains than that of soil. It was found that D_{min} slightly increased with soil plasticity for the Cretaceous soil deposits. The effect of soil plasticity on D_{min} was much less than the prediction by Andrus et al. (2003). Overall, the results from the laboratory testing program suggest that that plasticity index and geologic age alone are not dominant factors affecting the dynamic soil properties for older soil deposits. It is hypothesized that cementation is a possible dominant factor, however detailed evaluation of cementation in relation with shear modulus and damping is beyond the scope of this study.

5.2. Recommendations

Data from this study can be used directly to perform site-specific site response analysis for Site A and Site B with the recommendation to perform sensitivity analyses to account for the uncertainty in the following:

1. ***Variation of V_s profiles obtained from a specific method.*** This uncertainty is related to variability in data analysis utilized for different method of testing. For example, several possible V_s models can be obtained from each of the surface geophysical methods. This is because the data analysis depends on knowledge of the geological and geotechnical information at a site and data interpretation performed by data analysts. Sensitivity analysis should be conducted to account for the range of possible profiles.
2. ***Variation of V_s profiles obtained from different methods*.** High spatial variation was observed, especially at Site A. A lower average V_s was observed for the top 200 ft obtained by the surface geophysical methods compared to that of the P-S suspension logging method. Sensitivity analysis should be conducted to account for the V_s profiles from different methods of testing.

3. ***Depth to the B-C boundary.*** The P-S logging method did not provide V_s profiles beyond the bottom of the borehole at Site A and Site B, and the depth to the B-C boundary was not identified at either site. The depth and characteristics of V_s profiles from the bottom of the borehole to the projected B-C boundary should be studied as part of the sensitivity analysis.
4. ***Variation of dynamic behaviors (shear modulus and damping curves) of deep sediment.*** The data generated in this report can be readily used for the sites investigated herein. However, the data are limited to depths where the samples were obtained. Use of the shear modulus and damping curves for other depths and other sites requires careful interpretation of soil boring logs. Soil types and index properties should be carefully evaluated to use predictive curves.
5. ***Interbedded rock and cemented layers.*** The presence of rock layers such as limestone at Site B and/or relative thin layers of highly cemented soils should be evaluated to assess their impact on the site response analysis.

For future deep borehole investigations, it is recommended that samples of rock and cemented soils be routinely collected from sites and tested to the extent possible. Laboratory testing should be performed to determine the dynamic behaviors using both resonant column and torsional shear testing for a wide range of strains in order to evaluate the effects of test frequency on low-strain damping.

Based on the results herein, the predictive curves for shear modulus and damping curves suggested by Vucetic and Dobry (1991) and Andrus et al. (2003) can be used for Quaternary deposits. However, these equations are not recommended for Tertiary and Cretaceous deposits because this study showed that soil plasticity and geologic age alone are not dominant factors affecting the dynamic soil properties for older soil deposits, particularly for those samples with cementation.

5.3. Implementation Plan

The following data were obtained in this project and are available for immediate implementation:

1. Soil boring logs for Site A in Conway and Site B in Andrews are summarized in Figs. 4.1 and 4.2, respectively. Additional details are available in Appendix A.
2. Shear wave velocity profiles developed from different methods of testing for each site are shown in Figs. 4.6 and 4.9. Details of the methodology and data analysis to develop each profile are available in Appendices A, B, and C for P-S logging method and MASW-SASW methods, MASW-MAM method and FWS method, respectively. Comparisons of these profiles along with the detailed discussions are included in this report in Section 4.3.
3. Detailed geological information and visual observation of soils and rocks are available in this report and Appendix D.
4. Soil index properties data and soil classifications are available in Appendix E

5. Shear modulus and damping curves and model parameters for the development of these curves are provided in this report in Section 4.4 and data is included in Appendix F. This information can be used for site response analyses.

5.4. Future Research Needed

Based on the findings of this study, the following research needs were identified:

1. This study makes clear that empirical relationships based on soil plasticity and geologic age do not provide an accurate prediction of the shear modulus and damping curves. Impacts of cemented layers on site response analyses are not clear and should be examined. Importantly, detailed evaluation of cementation and other factors in relation with shear modulus and damping should be investigated in order to develop more accurate predictive models for SCDOT engineers and contractors.
2. Given the high variability in parameters observed within and between the sites studied herein, additional deep V_s profiles, with extensive sampling and laboratory testing to obtain shear modulus and damping curves, need to be obtained for more locations in the South Carolina Coastal Plain.
3. The surface wave methods show promising results, but require further studies to examine the testing procedures, data analyses protocols, and impacts on the results of site response analyses.

References

Andrus, R. D., Hayati, H., & Mohanan, N. P. (2009). Correcting Liquefaction Resistance for Aged Sands Using Measured to Estimated Velocity Ratio. Journal of Geotechnical and Geoenvironmental Engineering,135(6), 735-744.

Andrus, R. D., Ravichandran, N., Aboye, S. A., Bhuiyan, A. H., & Martin, J. R. (2014). Seismic Site Coefficients and Acceleration Design Response Spectra Based on Conditions in South Carolina (No. FHWA-SC-14-02). South Carolina. Dept. of Transportation.

Andrus, R. D., Zhang, J., Ellis, B. S., & Juang, C. H. (2003). Guide for Estimating the Dynamic Properties of South Carolina Soils for Ground Response Analysis (No. FHWA-SC-03-07,).

Bonnefoy-Claudet, S. (2004). Nature du bruit de fond sismique: implications pour les études des effets de site (Doctoral dissertation, Université Joseph Fourier (Grenoble).

Camp, W.M. (2018) Personal Communication. 17 April.

Chapman, M. C., & Talwani, P. (2006). Seismic Hazard Mapping for Bridge and Highway Design in South Carolina (No. FHWA-SC-06-09).

Chapman, M. C., Martin, J. R., Olgun, C. G., & Beale, J. N. (2006). Site-Response Models for Charleston, South Carolina, and Vicinity Developed from Shallow Geotechnical Investigations. Bulletin of the Seismological Society of America, 96(2), 467-489.

Christopher, R. A., & Prowell, D. C. (2002). A Palynological Biozonation for the Maastrichtian Stage (Upper Cretaceous) of South Carolina, USA. Cretaceous Research, 23(6), 639-669.

Darendeli, M. B. (2001). Development of a New Family of Normalized Modulus Reduction and Material Damping Curves. Ph. D. Dissertation, The University of Texas at Austin.

Doar, R. W. (2018) Personal Communication. 12 March.

F&ME Consultants (2017). Geotechnical Base Line Report US 21 (Sea Island Parkway) Bridge over Harbor River Beaufort County, South Carolina, SCDOT Project ID: P026862.

Fallaw, W. C., & Price, V. (1995). Stratigraphy of the Savannah River Site and Vicinity. Southeastern Geology, 35(1), 21-58.

Gellici, J. (2019) Personal Communication. 31 May.

GEOvision (2008). P-S Suspension Logging Borehole G-B-1, I-73 Project Little Pee Dee River near Mullins, South Carolina, Report 8451-01.

GEOvision (2010a). Suspension PS velocities Boring GEI-4 and GEI-5 Back Gate Bridge, Murrells Inlet, SC, Report 9459-01.

Hwang, S. K. (1997). Investigation of the Dynamic Properties of Natural Soils. Ph. D. Dissertation, The University of Texas at Austin.

Isenhower, W. M. (1979). Torsional Simple Shear/Resonant Column Properties of San Francisco Bay Mud. Ph. D. Dissertation, The University of Texas at Austin.

Ishibashi, I., & Zhang, X. (1993). Unified Dynamic Shear Moduli and Damping Ratios of Sand and Clay. Soils and Foundations, 33(1), 182-191.

Jeon, S. Y. (2008). Dynamic and Cyclic Properties in Shear of Tuff Specimens from Yucca Mountain, Nevada, Ph. D. Dissertation, The University of Texas at Austin.

Kavazanjian Jr, E., Matasović, N., Hadj-Hamou, T., & Sabatini, P. J. (1997). Design Guidance: Geotechnical Earthquake Engineering for Highways, Volume I, Design Principles. Geotechnical Engineering Circular No. 3, Report FHWA-SA-97, 76.

Kim, D. S. (1991). Deformational Characteristics of Soils at Small to Intermediate Strains from Cyclic Test. Ph. D. Dissertation, The University of Texas at Austin.

Kimball, C. V., & Marzetta, T. L. (1984). Semblance Processing of Borehole Acoustic Array Data. Geophysics, 49(3), 274-281.

Lachetl, C., & Bard, P. Y. (1994). Numerical and Theoretical Investigations on the Possibilities and Limitations of Nakamura's Technique. Journal of Physics of the Earth, 42(5), 377-397.

Lermo, J., & Chávez-García, F. J. (1993). Site Effect Evaluation Using Spectral Ratios with Only One Station. Bulletin of the Seismological Society of America, 83(5), 1574-1594.

Lodde, P. F. (1982). Shear Moduli and Material Damping of San Francisco Bay Mud. MS Thesis.

Minear, J. W. (1986). Full Wave Sonic Logging—a Brief Perspective: Transactions of the Society of Professional Well Log Analysts 27th Annual Logging Symposium. Paper AAA.

Ni, S. H. (1987). Dynamic Properties of Sand under True Triaxial Stress States from Resonant Column/Torsional Shear Tests. Ph. D. Dissertation, The University of Texas at Austin.

Nystrom, P. G., & Maybin, A. H. (2005). Generalized Geologic Map of South Carolina 2005. South Carolina State Documents Depository.

Rix, G. J., & Leipski, E. A. (1991). Accuracy and Resolution of Surface Wave Inversion in Geotechnical Special Publication no 29. Recent Advances in Instrumentation, Data Acquisition and Testing in Soil Dynamics, 17-32.

Rix, G. J., & Meng, J. (2005). A Nonresonance Method for Measuring Dynamic Soil Properties. Geotech. Test. J., 281, 1–8.

Ruttithivaphanich P. & Sasanakul I. (2019). Frequency Effects on Low-Strain Shear Modulus and Damping for Natural Clays and Silts. Geo-Congress 2019, Philadelphia, Pennsylvania.

S&ME (2015). Geotechnical Base Line Report Port Access Road North Charleston, South Carolina, S&ME Project No. 1131-08-554.

Sasanakul, I. (2005). Development of an Electromagnetic and Mechanical Model for a Resonant Column and Torsional Shear Testing for Soils. Ph. D. Dissertation, Utah State University.

Sasanakul, I., & Bay, J. (2008), Stress Integration Approach in Resonant Column and Torsional Shear Testing for Soils, ASCE Journal of Geotechnical and Geoenvironmental Engineering, Vol. 134, No. 12, December, pp. 1757-1762.

Sasanakul, I., & Bay, J. A. (2010). Calibration of Equipment Damping in a Resonant Column and Torsional Shear Testing Device. Geotechnical Testing Journal, 33(5), 363-374.

Seed, H. B., & Idriss, I. M. (1981). Evaluation of Liquefaction Potential Sand Deposits Based on Observation of Performance in Previous Earthquakes. In ASCE National Convention (MO), pp. 481-544.

Seed, H. B., Wong, R. T., Idriss, I. M., & Tokimatsu, K. (1986). Moduli and Damping Factors for Dynamic Analyses of Cohesionless Soils. Journal of Geotechnical Engineering, 112(11), 1016-1032.

Self-Trail, J. M., Christopher, R. A., & Prowell, D. C. (2002). Evidence for Large-Scale Reworking of Campanian Sediments into the Upper Maastrichtian Peedee Formation at Burches Ferry, South Carolina. Southeastern Geology, 41(3), 145-158.

SESAME European project, (2004). Guidelines for the Implementation of the H/V Spectral Ratio Technique on Ambient Vibrations: Measurements, Processing and Interpretation. Deliverable D23.12.

Stokoe II KH, Wright GW, James AB, & Jose MR (1994) Characterization of Geotechnical Sites by SASW Method. In Woods, RD, Ed., Geophysical Characterization of Sites: Oxford Publ.

Stokoe, K. H., Darendeli, M. B., Andrus, R. D., & Brown, L. T. (1999). Dynamic Soil Properties: Laboratory, Field and Correlation Studies. In Proceednings of the 2nd International Conference on Earthquake Geotechnical Engineering, pp. 811-846.

Stokoe, K. H., Hwang, S. K., Lee, J. K., & Andrus, R. D. (1995). Effects of Various Parameters on the Stiffness and Damping of Soils at Small to Medium Strains. Proceedings of the International Symposium, 12-14.

Sun, J. I., Golesorkhi, R., & Seed, H. B. (1988). Dynamic Moduli and Damping Ratios for Cohesive Soils. Berkeley: Earthquake Engineering Research Center, University of California.

Vucetic, M., & Dobry, R. (1991). Effect of Soil Plasticity on Cyclic Response. Journal of Geotechnical Engineering, 117(1), 89-107.

Zhang, J., Andrus, R. D., Juang, C. H. (2005). Normalized Shear Modulus and Material Damping Ratio Relationships. Journal of Geotechnical and Geoenvironmental Engineering, 131(4), 453-464.

Zhang, J., Andrus, R. D., Juang, C. H. (2008). Model Uncertainty in Normalized Shear Modulus and Damping Relationships. Journal of Geotechnical and Geoenvironmental Engineering, 134(1), 24-36.